Inorganic Chemistry

Article

pubs.acs.org/IC

Nitroimidazole-Containing H_2dedpa and H_2*CHX*dedpa Derivatives as Potential PET Imaging Agents of Hypoxia with ^{68}Ga

Caterina F. Ramogida,[†,‡] Jinhe Pan,[§] Cara L. Ferreira,[∥] Brian O. Patrick,[†] Karla Rebullar,[†] Donald T. T. Yapp,[§] Kuo-Shyan Lin,[§] Michael J. Adam,[‡] and Chris Orvig*[,†]

[†]Medicinal Inorganic Chemistry Group, Department of Chemistry, University of British Columbia, 2036 Main Mall, Vancouver, British Columbia V6T 1Z1, Canada

[‡]TRIUMF, 4004 Wesbrook Mall, Vancouver, British Columbia V6T 2A3, Canada

[§]BC Cancer Agency, 675 West 10th Avenue, Vancouver, British Columbia V5Z 1L3, Canada

[∥]Nordion, 4004 Wesbrook Mall, Vancouver, British Columbia V6T 2A3, Canada

Supporting Information

ABSTRACT: ^{68}Ga is an attractive radiometal for use in positron emission tomography (PET) imaging. The success of ^{68}Ga-based agents is dependent on a chelator that exhibits rapid radiometal incorporation, and strong kinetic inertness to prevent transchelation of ^{68}Ga in vivo. The linear chelating agents H_2dedpa (1,2-[[6-carboxypyridin-2-yl]methylamino]-ethane) and H_2*CHX*dedpa (*CHX* = cyclohexyl/cyclohexane) (N_4O_2) have recently been developed that bind Ga^{3+} quickly and under mild conditions, ideal properties to be incorporated into a ^{68}Ga PET imaging agent. Herein, nitroimidazole (NI) derivatives of H_2dedpa and H_2*CHX*dedpa to investigate specific targeting of hypoxic tumor cells are investigated, given that NI can be reduced and retained exclusively in hypoxic cells. Nine *N*,*N*′-bis-alkylated derivatives of H_2dedpa and H_2*CHX*dedpa have been synthesized; they have been screened for their ability to bind gallium, and cyclic voltammetry of nonradioactive complexes was performed to probe the redox cycling mechanism of NI. The compounds were radiolabeled with ^{67}Ga and ^{68}Ga and show promising radiolabeling efficiencies (>99%) when labeled at 10^{-5} M for 10 min at room temperature. Moreover, stability studies (via *apo*-transferrin challenge, 37 °C) show that the ^{67}Ga complexes exhibit exceptional stability (86−99% intact) after 2 h. In vitro uptake studies under hypoxic (0.5% O_2) and normoxic (21% O_2) conditions in three cancerous cell lines [HT-29 (colon), LCC6^{HER-2} (breast), and CHO (Chinese hamster ovarian)] were performed. Of the four H_2dedpa or H_2*CHX*dedpa NI derivatives tested, all showed preferential uptake in hypoxic cells compared to normoxic cells with hypoxic/normoxic ratios as high as 7.9 ± 2.7 after 120 min. The results suggest that these novel bis-alkylated NI-containing H_2dedpa and H_2*CHX*dedpa ligands would be ideal candidates for further testing in vivo for PET imaging of hypoxia with ^{68}Ga.

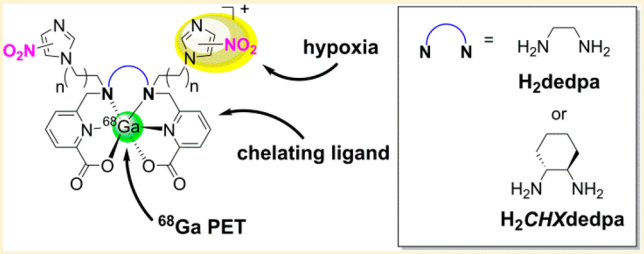

INTRODUCTION

Hypoxia, a condition defined by an insufficient oxygen supply to support metabolism, is an important characteristic in many diseases, playing a role in stroke, heart attack, and oncology.[1,2] It has specific consequences in oncology because solid tumors that are hypoxic tend to be more aggressive and resistant to radiotherapy and chemotherapy compared to well-oxygenated cells (normoxia).[3−8] As a consequence, hypoxia can greatly compromise a patient's survival outcome. For this reason, hypoxia is a high-priority target where identification of hypoxic regions in tumors would allow appropriate therapies to be chosen for each patient, presumably improving patient prognosis. The class of compounds containing nitroimidazoles (NIs) is among the most popular strategy used for tracking and imaging hypoxia. NIs have the ability to be reduced and retained exclusively in hypoxic cells via direct competition with intracellular oxygen concentration. The accepted mechanism of action commences with the NI tracer entering the cell; once inside the cell, one-electron reduction to form the nitro radical anion ($NO_2^{\bullet-}$) can occur in all cells (normoxic and/or hypoxic).[1,4,6,9,10] In normoxic cells, intracellular oxygen will compete for the electron and the radical anion can be backoxidized to form the native NO_2 compound, which can subsequently leave the cell freely. In hypoxic cells, the inherent insufficient oxygen supply results in the incapability of backoxidation of the $NO_2^{\bullet-}$ radical; hence, the nitro radical can be further reduced to form reactive species that can covalently bind to macromolecules intracellularly; the NI tracer is now irreversibly trapped inside the hypoxic cell (Figure 1).[1,4,6,9,10]

This bioreductive trapping mechanism has been exploited in several ^{18}F-labeled 2-NI clinical tracers such as fluoromisonidazole (F-MISO)[13,14] and, more recently, fluoroazomycin

Received: March 10, 2015
Published: April 30, 2015

DOI: 10.1021/acs.inorgchem.5b00554
Inorg. Chem. 2015, 54, 4953−4965

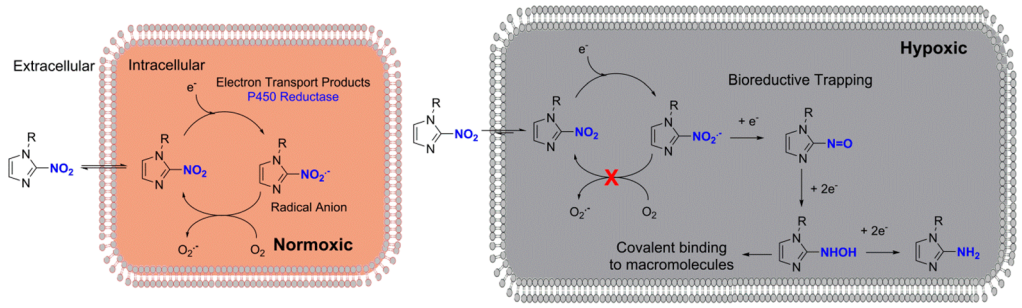

Figure 1. Accepted trapping mechanism of NIs in hypoxic cells.[1,11,12]

arabinofuranoside (FAZA)[15,16] and etanidazole pentafluoride (EF5)[17−19] used in positron emission tomography (PET) imaging of hypoxia (Figure 2). The relatively high lipophilicity

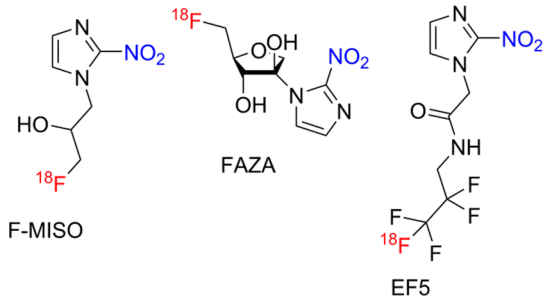

Figure 2. ^{18}F-labeled 2-NI hypoxia tracers F-MISO, EF5, and FAZA.

of many ^{18}F-labeled 2-NI tracers (log P = 0.43 for F-MISO[20]) allows for facile penetration through the cell membrane; however, as a consequence, clearance from a nontarget tissue is slow, resulting in high liver uptake and low tumor-to-background ratios.[8] More hydrophilic tracers that are cleared rapidly from a nontarget tissue would be of great interest.

The positron emitter ^{68}Ga has been proposed as an alternative to ^{18}F because it has a high positron branching ratio (89%; $E_{\beta^+\,max}$ = 1.9 MeV)[21] and a comparably short half-life ($t_{1/2}$ = 67.7 min compared to 118 min for ^{18}F). Unlike the "organic" nuclide, ^{68}Ga can be incorporated into a radiotracer via a facile and efficient coordination complex. Moreover, ^{68}Ga is produced in a commercially available ^{68}Ge/^{68}Ga generator system; the half-life of the parent ^{68}Ge ($t_{1/2}$ = 270.95 days) allows the generator to be used for up to 1 year, with two or three elutions per day providing a very cost-effective means of supplying isotope while obviating the need for an on-site cyclotron.[22−26]

Naturally, a hypoxia tracer incorporating ^{68}Ga would be of great interest. As a result, the hypoxia targeting moiety NI has been successfully incorporated into the strong gallium chelators 1,4,7-triazacyclononane-1,4,7-triacetic acid (NOTA) and 1,4,7,10-tetraazacyclododecane-1,4,7,10-tetraacetic acid (DOTA) with moderate-to-good results.[27−29] Recently, our group has investigated an acyclic hexadentate (N_4O_2) chelator, 1,2-[[6-carboxypyridin-2-yl]methylamino]ethane (H_2dedpa), which displays ideal properties for gallium(III) chelation and elaboration into a radiopharmaceutical for ^{68}Ga PET imaging,[30] such as mild and efficient radiolabeling of gallium isotopes [radiochemical yield (RCY) >99%; 10 min at room temperature] exceptionally high thermodynamic stability constants with gallium(III) [log K_{ML} = 28.11(8)], and forms complexes of promising kinetic inertness in vitro. More recently, we have investigated the chiral derivative H_2*CHX*dedpa (*CHX* = cyclohexyl/cyclohexane), which incorporates a 1*R*,2*R*-*trans*-cyclohexanediamine backbone in place of the ethylenediamine bridge to form a ligand with an augmented preorganization of donor atoms, which restricts the flexibility around the coordinating atoms in order to form metal complexes of even higher kinetic inertness. Much like its achiral analogue H_2dedpa, H_2*CHX*dedpa forms gallium(III) complexes of exceptionally high thermodynamic stability [log K_{ML} = 27.61(8)] and exhibits even higher in vitro kinetic inertness.[31] Herein, we report H_2dedpa and H_2*CHX*dedpa chelating ligands that have been functionalized with NI moieties as potential PET imaging agents of hypoxia with ^{68}Ga. The chelating ligands have been functionalized via their secondary amines with alkylation using either an ethyl or a propyl linker and an imidazole ring with the nitro group in the 2, 5, or 4 position (Figure 3). The synthesis and characterization of pro-ligands and "cold" metal complexes, electrochemical studies to determine the redox behaviors of the NI moieties, radiolabeling experiments with both ^{67}Ga and ^{68}Ga, determination of partition coefficients (log $D_{7.4}$), in vitro stability, and in vitro cell uptake under hypoxic versus normoxic conditions were determined. The studies were used collaboratively to determine the feasibility of these novel H_2dedpa-*N*,*N*′-alkyl-NI or

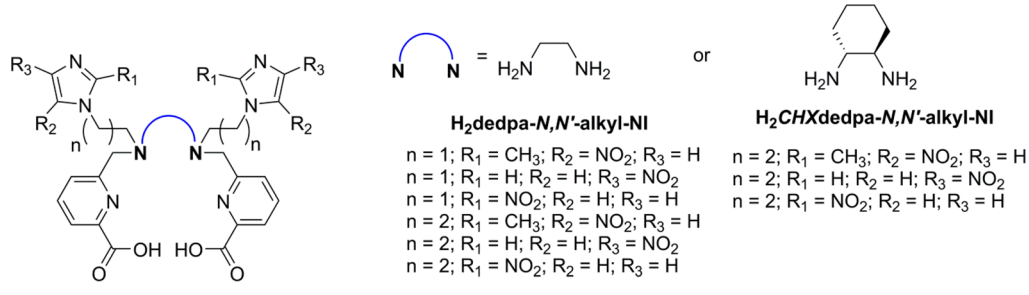

Figure 3. General structures of NI-containing H_2dedpa and H_2*CHX*dedpa ligands investigated in this work.

DOI: 10.1021/acs.inorgchem.5b00554
Inorg. Chem. 2015, 54, 4953−4965

Scheme 1. Synthesis of 1-(ω-Bromoalkyl)nitroimidazoles (7−12)

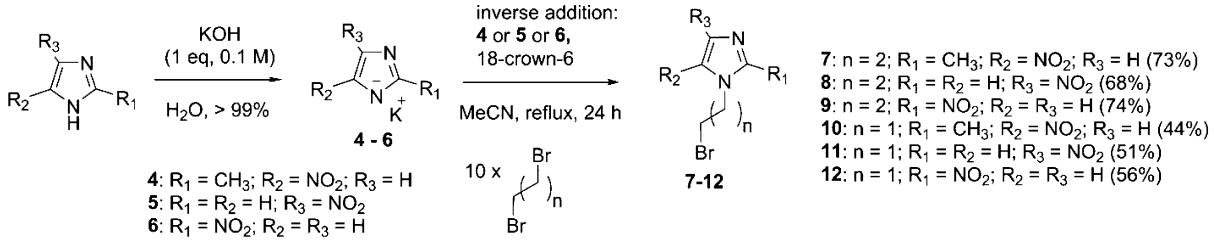

Scheme 2. Synthesis of H_2dedpa-*N,N′*-alkyl-NIs (19−24) and H_2*CHX*dedpa-*N,N′*-propyl-NIs (28−30)

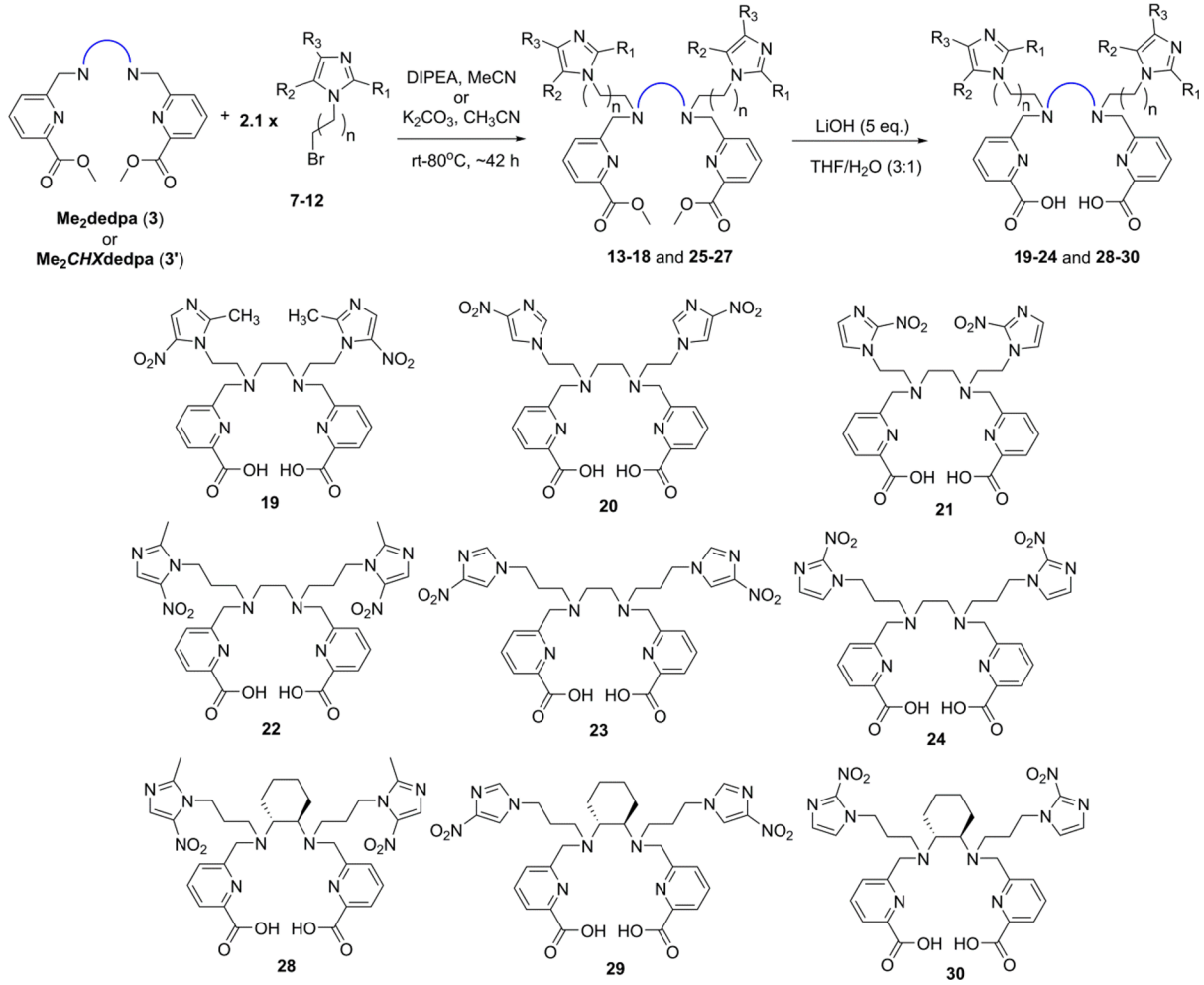

H_2*CHX*dedpa-*N,N′*-alkyl-NI agents as chelating ligands for PET imaging of hypoxia with ^{68}Ga.

RESULTS AND DISCUSSION

Synthesis and Characterization. A small library of NI-containing H_2dedpa or H_2*CHX*dedpa pro-ligands containing varying alkyl chain linker length (ethyl or propyl) and varying substitution around the imidazole ring (2-, 4-, or 5-NI) were synthesized. Changing the linker length between the ligand and NI targeting vector can serve two purposes: (1) to make compounds of varying lipophilicity—lipophilic molecules can more easily pass through the cell membrane; however, very lipophilic compounds have a tendency to accumulate in the liver, causing poor biodistribution profiles in vivo; thus, a balance must be found; (2) to increase the distance between the metal-bound chelate and targeting vector in order to reduce the chance of interference between the two independent parts of the radiotracer—the targeting vector/linker should not affect the metal-binding ability of the chelate, and the metal complex should not affect the targeting vector's ability to be reduced and retained intracellularly. Changing the substitution of the nitro group on the imidazole ring alters the reduction potential of the nitro radical; because the retention of NI is dependent on the one-electron redox, this would subsequently alter the compound's ability to be entrapped inside hypoxic tissue.

Methyl ester protected Me_2dedpa (**3**) or Me_2*CHX*dedpa (**3′**) was prepared via a previously published method from our group.[31,32] Bromoalkylating agents **7**−**12** were prepared using a previously reported synthesis of similar analogues (Scheme 1).[33] Alkylation of Me_2dedpa with the ethyl-linked NIs (**10**−**12**) was poor yielding (10−23%) compared to alkylation with the propyl derivatives (**7**−**9**; 30−69%; Scheme 2). This result is

DOI: 10.1021/acs.inorgchem.5b00554
Inorg. Chem. 2015, 54, 4953−4965

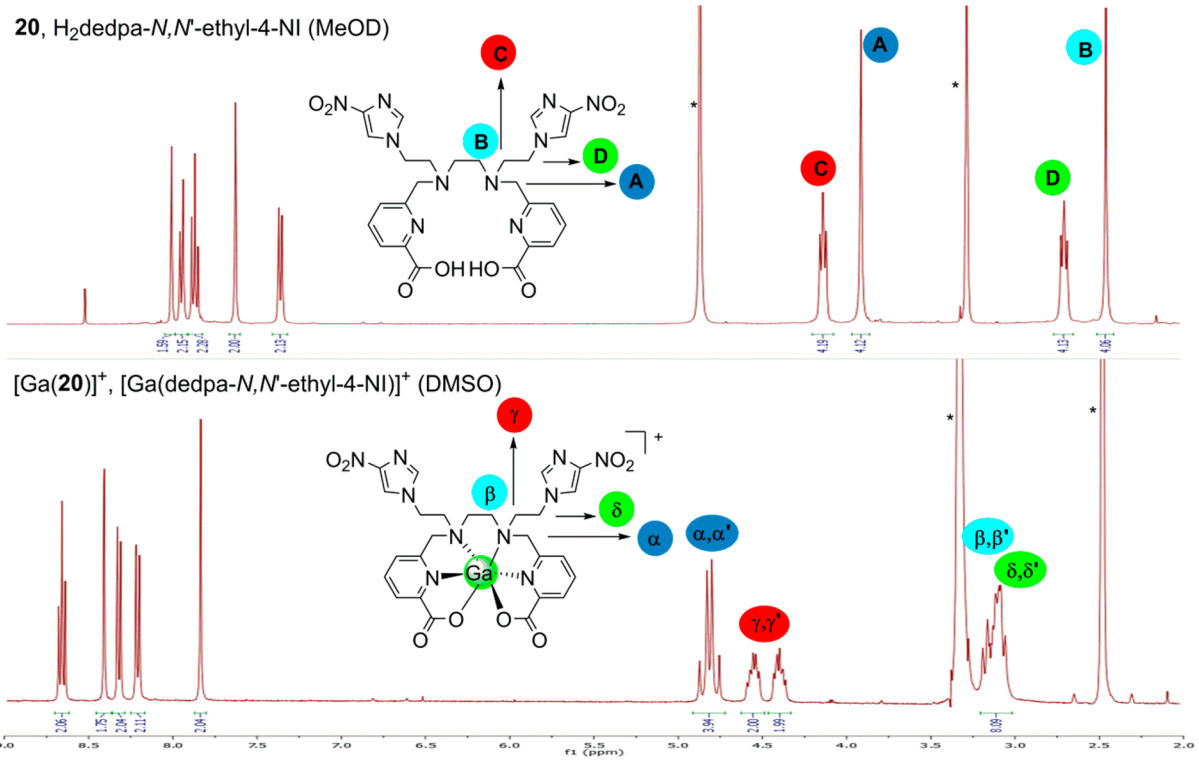

Figure 4. ^{1}H NMR spectrum at 400 MHz of (top) H_2dedpa-*N*,*N*′-ethyl-4-NI (**20**) and (bottom) [Ga(**20**)][ClO_4] highlighting diastereotopic splitting upon gallium chelation. Asterisks indicate residual solvent peaks.

due to the intrinsic electronics of the NI ring, which destabilizes the δ^+ charge on the electrophilic carbon α to the bromine atom; hence, the propyl-linked derivatives were less affected by the destabilization of partial charge due to the NI's relative distance to the electrophilic carbon and resulted in higher yielding syntheses. Considering this and the fact that the ethyl-linked derivatives may impose more of a steric hindrance around the metal-binding cavity, only the propyl-linked analogues of *CHX*dedpa^{2-} were synthesized (Scheme 2). Six H_2dedpa derivatives with either an ethyl or a propyl linker and different substitution around the imidazole ring (**19**–**24**) and three H_2*CHX*dedpa derivatives with a propyl linker and varying substitution of the imidazole ring (**28**–**30**) were synthesized and characterized.

After synthesis, all nine pro-ligands were allowed to complex with "cold" (nonradioactive) gallium(III) and characterized by ^{1}H/^{13}C NMR, mass spectrometry (MS), and, when successful, X-ray crystallography. ^{1}H NMR spectra of the H_2dedpa-*N*,*N*′-alkyl-NI pro-ligands exhibited C_{2v} symmetry, with only half the resonances present. While the C_2 symmetry is retained (only half the resonances present) in the metal complexes, diastereotopic splitting of the methylene hydrogen atoms alpha to the pyridine ring, hydrogen atoms in the ethylenediamine bridge, and hydrogen atoms of the ethylene or propylene linker is observed in the ^{1}H NMR spectra of the [Ga(dedpa-*N*,*N*′-alkyl-NI)]$^+$ complexes and is used as a diagnostic handle to confirm successful metal coordination (see Figure 4 for representative spectra). The intrinsically chiral H_2*CHX*dedpa-*N*,*N*′-alkyl-NI pro-ligands already exhibit diastereotopic splitting of hydrogen atoms alpha to the chiral cyclohexane ring in the ^{1}H NMR spectra; nonetheless, shifts in the hydrogen resonances are observed in the [Ga(*CHX*dedpa-*N*,*N*′-alkyl-NI)]$^+$ complexes, which were used to confirm gallium(III) chelation; in addition, C_2 symmetry is conserved (Figure S1 in the Supporting Information, SI).

X-ray-quality crystals of [Ga(dedpa-*N*,*N*′-ethyl-2-NI)][ClO_4] ([Ga(**21**)][ClO_4]; Figure 5) and [Ga(dedpa-*N*,*N*′-propyl-4-NI)][ClO_4] ([Ga(**23**)][ClO_4]; Figure 6) were obtained through slow evaporation in water/acetonitrile (~1:4). Qualitative examination of the obtained structures confirms that the N_4O_2 coordination sphere of a native dedpa^{2-} ligand is retained, while the two NI targeting vectors are pointed in opposite directions, away from the metal-binding sphere. Only minor differences were found upon close quantitative

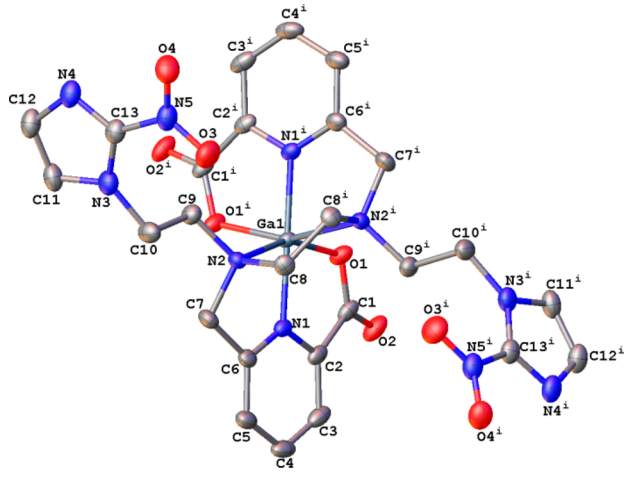

Figure 5. Solid-state structure of the cation in [Ga(dedpa-*N*,*N*′-ethyl-2-NI)][ClO_4]. Counterions are omitted for clarity. Ellipsoids are drawn with 50% probability. Superscript i refers to the symmetry operation $-^1/_2 - x, -^3/_2 - y, +z$.

DOI: 10.1021/acs.inorgchem.5b00554
Inorg. Chem. 2015, 54, 4953–4965

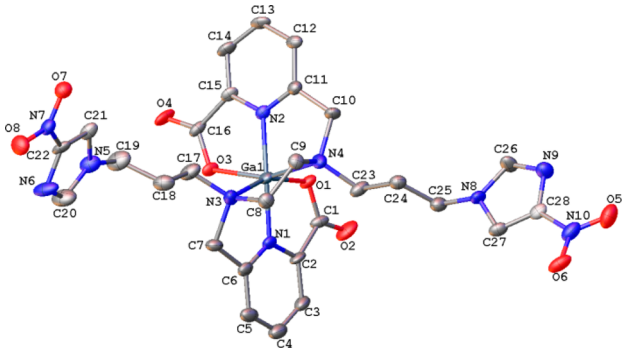

Figure 6. Solid-state structure of the cation in the major disordered fragment of [Ga(dedpa-*N,N′*-propyl-4-NI)][ClO_4]. Counterions are omitted for clarity. Ellipsoids are drawn with 50% probability.

comparison of relevant bond lengths and angles of the two novel [Ga(dedpa-*N,N′*-alkyl-NI)]$^+$ solid-state structures to the previously reported [Ga(dedpa)]$^+$ complex[30] (Table 1). The largest difference in relevant Ga−L bond lengths between [Ga(**21**)]$^+$ and the "unfunctionalized" [Ga(dedpa)]$^+$ complex is 0.10 Å, which arose from both Ga−N_{en} bonds in the *N,N′*-functionalized complex being longer than those in [Ga(dedpa)]$^+$. A comparison of all other Ga−L bonds yielded differences of much less than 0.10 Å. The largest difference in the relevant L−Ga−L bond angles is 5.6°. A comparison of the propyl-linked complex, [Ga(**23**)]$^+$, to the "unfunctionalized" [Ga(dedpa)]$^+$ revealed very minor differences in the relevant Ga−L bond lengths. The largest difference of 0.08 Å arises from one of the Ga−$O_{pyr\text{-}COO}$ bonds in [Ga(**23**)]$^+$ being longer than the analogous bond in the [Ga(dedpa)]$^+$ structure, and largest L−Ga−L bond angle difference between the two complexes is only 6.6°. The lack of major changes in the solid-state structures of these novel *N,N′*-functionalized Ga-dedpa derivatives bodes well for their retention of stability in vitro compared to the unfunctionalized Ga-dedpa; however, caution must be taken upon comparison of solid-state data to reflect solution-state properties, and in vitro stability assays are better predictors of kinetic inertness (vide infra).

Electrochemistry. The mechanism of intracellular NI trapping is directly dependent on the reduction ability and reduction potential (E_{red}) of the nitro group. Hence, the redox behaviors of the [Ga((*CHX*)dedpa-*N,N′*-alkyl-NI)]$^+$ complexes were determined by cyclic voltammetry in both aqueous (0.1 M KCl, pH 7; Figure S66 in the SI) and nonaqueous [dimethyl sulfoxide (DMSO) and 0.1 M tetrabutylammonium perchlorate (TBAP); Figure 7] conditions and compared directly with the clinically relevant agents F-MISO (2-NI) and metronidazole [METRO, 5-NI, 2-(2-methyl-5-nitro-1*H*-imidazol-1-yl)-ethanol].

The cyclic voltammograms (CVs) of F-MISO and METRO in nonaqueous solvent (DMSO, 0.1 M TBAP) exhibit one quasi-reversible couple at −0.993 and −1.283 V, respectively, which presumably arise from reduction of the nitro group (NO_2) to form a nitro radical ($NO_2^{\bullet-}$) upon falling potential sweep from 0 to approximately −2 V and back-oxidation to the initial nitro group upon increasing potential from approximately −2 to +1.3 V. These results are corroborated by previously reported values, which also show that F-MISO (2-NI) has a less negative (easier to reduce) reduction potential than other 5- or 4-NI compounds (such as METRO), with this difference being about 250 mV.[34,35] This trend is sustained with the novel Ga-dedpa-NI and Ga-*CHX*dedpa-NI complexes [Ga(**19**−**24**) or Ga(**28**−**30**)], which also show one major quasi-reversible couple (in DMSO) at approximately −1.05 V (for 2-NI compounds) or approximately −1.35 V (for 5- or 4-NI compounds) (Table 2 and Figure 7). Moreover, a CV of the Ga complex with the addition of exactly 1 equiv of ferrocene (Fc) results in a voltammogram with the redox couple due to the nitro group of the Ga-dedpa-NI compound being almost exactly twice in amplitude to the Fc/Fc$^+$ couple (Figure S65 in the SI), suggesting that both NI groups on the dedpa core are being reduced simultaneously and independently of each other. The addition of two "hypoxia trapping" groups on one

Table 1. Selected Bond Lengths (Å) and Angles (deg) in the Solid-State Structures of Gallium Complexes Compared to Previously Reported [Ga(dedpa)][ClO_4]

		[Ga(dedpa-*N,N′*-ethyl-2-NI)]$^+$		[Ga(dedpa-*N,N′*-propyl-4-NI)]$^+$	
	length (Å) of [Ga(dedpa)]$^+$ [a]	bond	length (Å) of [Ga(**21**)]$^+$	bond	length (Å) of [Ga(**23**)]$^+$
Ga−N_{pyr}	1.9868(16)	Ga−N1	1.980(2)	Ga−N1	1.985(9)
Ga−N_{pyr}	1.9903(16)	Ga−N1^i	1.980(2)	Ga−N2	1.996(9)
Ga−N_{en}	2.1115(16)	Ga−N2	2.2172(19)	Ga−N3	2.177(3)
Ga−N_{en}	2.1132(16)	Ga−N2^i	2.2172(19)	Ga−N4	2.183(2)
Ga−$O_{pyr\text{-}COO}$	1.9708(13)	Ga−O1	1.9626(16)	Ga−O1	2.038(12)
Ga−$O_{pyr\text{-}COO}$	1.9828(13)	Ga−O1^i	1.9626(16)	Ga−O3	2.068(10)
		[Ga(dedpa-*N,N′*-ethyl-2-NI)]$^+$		[Ga(dedpa-*N,N′*-propyl-4-NI)]$^+$	
	angle (deg) of [Ga(dedpa)]$^+$	angle	angle (deg) of [Ga(**21**)]$^+$	angle	angle (deg) of [Ga(**23**)]$^+$
O_{COO}−Ga−O_{COO}	101.39(6)	O1−Ga−O1^i	98.52(10)	O1−Ga−O3	94.8(7)
O_{COO}−Ga−N_{pyr}	94.02(6)	O1^i−Ga−N1	98.25(7)	O3−Ga−N1	95.4(4)
O_{COO}−Ga−N_{pyr}	79.64(6)	O1^i−Ga−N1^i	81.03(8)	O3−Ga−N2	77.9(3)
N_{pyr}−Ga−N_{pyr}	170.97(6)	N1−Ga−N1^i	178.91(11)	N1−Ga−N2	168.3(3)
O_{COO}−Ga−N_{en}	94.78(6)	O1−Ga−N2^i	93.41(7)	O3−Ga−N3	95.1(4)
O_{COO}−Ga−N_{en}	155.64(6)	O1−Ga−N2	156.60(7)	O3−Ga−N4	158.3(3)
N_{pyr}−Ga−N_{en}	109.11(6)	N1−Ga−N2^i	103.47(7)	N2−Ga−N3	108.0(2)
N_{pyr}−Ga−N_{en}	78.15(6)	N1^i−Ga−N2^i	77.36(7)	N1−Ga−N3	81.9(2)
N_{en}−Ga−N_{en}	83.12(6)	N2^i−Ga−N2	83.05(10)	N3−Ga−N4	84.05(9)

[a]Values from the previously reported [Ga(dedpa)][ClO_4] complex.[30]

DOI: 10.1021/acs.inorgchem.5b00554
Inorg. Chem. 2015, 54, 4953−4965

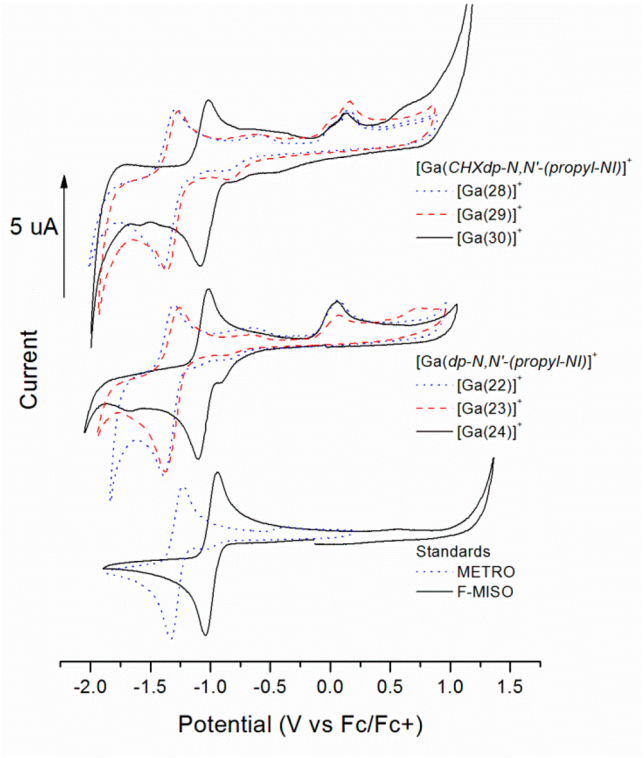

Figure 7. CVs of [Ga((*CHX*)dedpa-*N,N′*-alkyl-NI)]$^+$ complexes and standards in nonaqueous solvent (DMSO, 0.1 M TBAP, and 1−5 mM complex): [Ga(*CHX*dedpa-*N,N′*-propyl-NI)]$^+$ compounds (top), [Ga(dedpa-*N,N′*-propyl-NI)]$^+$ compounds (middle), and clinical standards F-MISO and METRO (bottom). 2-NI compounds (black), 5-NI compounds (blue dotted), and 4-NI compounds (red dashed). Legend: dp = dedpa; *CHX*dp = *CHX*dedpa.

radiotracer may increase the probability of successful entrapment in hypoxic cells; this hypothesis has also been suggested by others.[36,37]

The CVs of standards and complexes in aqueous media (water, 0.1 M KCl, pH 7) are very different, where F-MISO and METRO show one irreversible reduction at −0.681 and −0.807 V, respectively (Figure S67 in the SI and Table 3). Again, these results are corroborated with previously reported values for F-MISO and METRO in aqueous solvent.[34,35,38] The CV of the novel [Ga(dedpa-*N,N′*-propyl-NI)]$^+$ complexes also exhibited irreversible reduction with E_{red}^1 values of −0.780, −0.779, and −0.631 V for the 5-, 4-, and 2-NI compounds, respectively. The title [Ga(dedpa-*N,N′*-propyl-NI)]$^+$ compounds possess a larger

Table 3. Reduction Potentials (E_{red}) for Gallium Complexes and Standards F-MISO and METRO Obtained from Cyclic Voltammetry in Water (0.1 M KCl, pH 7, 1−5 mM Complex, vs Ag/AgCl)[a]

compound		E_{red}^1/V	E_{red}^2/V
METRO (5-NI)		−0.807	
[Ga(dp-*N,N′*-propyl-2-Me-5-NI)]$^+$	[Ga(**22**)]$^+$	−0.780	−1.133
[Ga(dp-*N,N′*-propyl-4-NI)]$^+$	[Ga(**23**)]$^+$	−0.779	−1.133
F-MISO (2-NI)		−0.681	
[Ga(dp-*N,N′*-propyl-2-NI)]+	[Ga(**24**)]$^+$	−0.631	−1.128

[a]dp = dedpa.

deviation from E_{red}^1 of the standards (F-MISO/METRO) in aqueous solvent compared to nonaqueous solvent; E_{red}^1 of the 4- or 5-NI gallium complexes were shifted positively 27 mV compared to the 5-NI clinical standard METRO, and E_{red}^1 of the 2-NI gallium complex was shifted 50 mV to the positive compared to the 2-NI clinical standard F-MISO. Moreover, all of the gallium complexes displayed a second irreversible reduction, E_{red}^2, at −1.13 V regardless of their nitro substitution.

The similarity between the redox behaviors of the standards F-MISO/METRO and the novel [Ga((*CHX*)dedpa-*N,N′*-alkyl-NI)]$^+$ complexes in nonaqueous solvent implies that linking the NI ring through an ethyl or propyl connection to the H_2dedpa or H_2*CHX*dedpa ligand backbone has no significant effect on the $E_{1/2}$ value of the nitro moiety, and the NIs should be seemingly uninhibited to undergo reduction in vitro and/or in vivo.

$^{67/68}$Ga Radiolabeling. Initial radiolabeling studies with both ^{67}Ga and ^{68}Ga were performed on all nine of the novel NI-containing pro-ligands **19**−**24** and **28**−**30**. γ-Emitter ^{67}Ga was used as a model for ^{68}Ga; because it has a longer half-life ($t_{1/2}$ = 3.3 days), it is a more convenient choice for in vitro testing. Initial results show that all H_2dedpa-*N,N′*-alkyl-NI and H_2*CHX*dedpa-*N,N′*-propyl-NI ligands were able to quantitatively bind gallium isotopes at 10^{-5} and 10^{-4} M (RCY >99%), respectively, in only 10 min at room temperature, displaying one sharp peak in the HPLC radiochromatogram. For the H_2dedpa-NI complexes, at ligand concentrations of 10^{-6} M or lower, incomplete labeling was observed (RCY ∼89% or less) when incubated for 10 min at room temperature. For the H_2*CHX*dedpa-*N,N′*-propyl-NI ligands, $^{67/68}$Ga labeling was partially incomplete (RCY 96%) at ligand concentrations of 10^{-5} M and reduced significantly (RCY 13%) at ligand concentrations of 10^{-6} M. In comparison, quantitative $^{67/68}$Ga

Table 2. E_{red}, E_{ox}, and Calculated $E_{1/2}$ Values for Gallium Complexes and Standards F-MISO and METRO Obtained from Cyclic Voltammetry in DMSO (0.1 M TBAP, 1−5 mM Complex, vs Fc/Fc$^+$)[a]

	compound		E_{red}/V	E_{ox}/V	$E_{1/2}$/V
2-NI	F-MISO (2-NI)		−1.045	−0.941	−0.993
	[Ga(dp-*N,N′*-propyl-2-NI)]$^+$	[Ga(**24**)]$^+$	−1.100	−1.021	−1.061
	[Ga(dp-*N,N′*-ethyl-2-NI)]$^+$	[Ga(**21**)]$^+$	−1.132	−1.067	−1.100
	[Ga(*CHX*dp-*N,N′*-propyl-2-NI)]$^+$	[Ga(**30**)]$^+$	−1.082	−1.013	−1.047
5- or 4-NI	METRO (2-Me-5-NI)		−1.334	−1.232	−1.283
	[Ga(*CHX*dp-*N,N′*-propyl-2-Me-5-NI)]$^+$	[Ga(**28**)]$^+$	−1.402	−1.291	−1.347
	[Ga(dp-*N,N′*-propyl-2-Me-5-NI)]$^+$	[Ga(**22**)]$^+$	−1.389	−1.300	−1.344
	[Ga(*CHX*dp-*N,N′*-propyl-4-NI)]$^+$	[Ga(**29**)]$^+$	−1.365	−1.266	−1.315
	[Ga(dp-*N,N′*-propyl-4-NI)]$^+$	[Ga(**23**)]$^+$	−1.363	−1.276	−1.319

[a]dp = dedpa; *CHX*dp = *CHX*dedpa.

DOI: 10.1021/acs.inorgchem.5b00554
Inorg. Chem. 2015, 54, 4953−4965

labeling (10 min at room temperature) of the unaltered proligands H_2dedpa[30] and H_2*CHX*dedpa[31] was accomplished at ligand concentrations as low as 10^{-7} and 10^{-5} M, respectively, suggesting that conversion of the secondary amines to tertiary amines via *N,N′*-alkylation with the corresponding 1-(*ω*-bromoalkyl)nitroimidazoles has impeded the labeling kinetics of the resultant ligands. Likely, extended reaction times or elevated temperatures are needed to achieve quantitative labeling at lower ligand concentrations, but these conditions were not tested.

The octanol/water partition coefficients (log $D_{7.4}$) of four selected ^{68}Ga complexes were also determined by mixing preformed ^{68}Ga tracer in equal amounts of phosphate-buffered saline (PBS; pH 7.4) and 1-octanol, separating the phases, and measuring the activity in aliquots of each phase. The lipophilicity of a compound plays an important role in the pharmacokinetics in vivo. For many ^{18}F-labeled hypoxia tracers such as F-MISO (log P = 0.43),[20] their relatively high lipophilicity limits tumor-to-background ratios and causes unwanted liver uptake. The novel Ga-dedpa-NI tracers are substantially more hydrophilic, with log $D_{7.4}$ values ranging between −2.16 and −2.76 (Table 4).

Table 4. Partition Coefficients (log $D_{7.4}$) of Selected ^{68}Ga Complexes

^{68}Ga complex		log $D_{7.4}$
[^{68}Ga(dedpa-*N,N′*-propyl-2-Me-5-NI)]$^+$	[Ga(**22**)]$^+$	−2.16 ± 0.29
[^{68}Ga(dedpa-*N,N′*-propyl-4-NI)]$^+$	[Ga(**23**)]$^+$	−2.63 ± 0.13
[^{68}Ga(dedpa-*N,N′*-propyl-2-NI)]$^+$	[Ga(**24**)]$^+$	−2.76 ± 0.19
[^{68}Ga(*CHX*dedpa-*N,N′*-propyl-2-NI)]$^+$	[Ga(**30**)]$^+$	−2.71 ± 0.12

***apo*-Transferrin Stability Studies.** The iron-transport protein, transferrin, has two sites for strong iron(III) binding, and because gallium(III) and iron(III) share many physical similarities, transferrin also has a strong affinity for gallium(III).[39] Consequently, *apo*-transferrin is a strong competitor for gallium(III) in vivo, and any chelate-bound gallium must be more thermodynamically stable and kinetically inert than gallium transferrin to prevent transchelation of radioactive gallium from the radiotracer to the endogenous protein. To investigate the stability of the ^{67}Ga complexes, a 2 h competition experiment in excess human *apo*-transferrin at 37 °C was performed. This assay is a preferred method to predict in vivo stability of the resultant gallium radiotracers. The results for the nine ^{67}Ga tracers are shown in Figure 8. With the exception of one ethyl-linked tracer, [^{67}Ga(dedpa-*N,N′*-ethyl-2-NI)]$^+$, which remained 68% intact, all other ^{67}Ga complexes exhibited very good to excellent stability, with the poorest being 86% intact and the highest being >99% intact after 2 h against *apo*-transferrin. These results indicate that the chelating ligands tested herein form kinetically inert gallium complexes, suggesting they would be good candidates for further testing in vitro and in vivo. A kinetically inert metal complex of an "open-chain" acyclic ligand is not a common manifestation; this fact further exemplifies the uniqueness of the H_2dedpa and H_2*CHX*dedpa scaffolds as promising gallium chelating ligands in radiopharmaceutical elaboration.

In Vitro Cell Uptake Studies. HT-29 (human colon), LCC6^{HER-2} (human breast), and CHO (Chinese hamster ovarian; data not shown) cancer cells were used in the in vitro cell uptake study of four ^{68}Ga(*CHX*)dedpa-*N,N′*-propyl-NI tracers: [^{68}Ga-**22**, -**23**, -**24**, or -**30**]$^+$. Cell uptake of all four

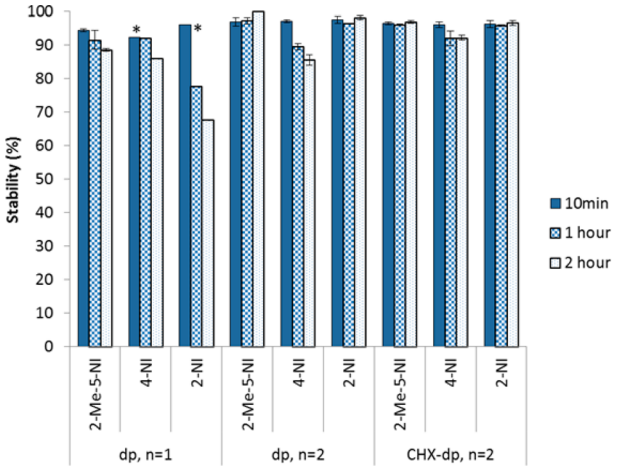

Figure 8. *apo*-Transferrin stability challenge assay of nine ^{67}Ga complexes at 37 °C. dp = dedpa; CHX-dp = *CHX*dedpa; n = 1, ethyl-linked; n = 2, propyl-linked; asterisks indicate single experiment performed; all others repeated in triplicate.

radiotracers in all three cell lines was performed under hypoxic (0.5% O_2) and normoxic (21% O_2) conditions and analyzed at time points of 10, 30, 60, and 120 min. All three cell lines showed significantly higher uptake of all four ^{68}Ga-dedpa tracers under hypoxic conditions compared to normoxic conditions after 30−60 min (Figure 9). The largest jump in uptake under hypoxic conditions occurred between 30 and 60 min for all cell lines and tracers tested. Hypoxic/normoxic ratios in LCC6^{HER-2} cells were as high as 7.9 ± 2.7 (^{68}Ga-**24** at 120 min), 6.3 ± 2.4 (^{68}Ga-**22** at 60 min), 5.8 ± 2.7 (^{68}Ga-**23** at 60 min), and 6.5 ± 1.7 (^{68}Ga-**30** at 60 min). Hypoxic/normoxic ratios in HT-29 cells were highest after 60 min for all tracers: 5.5 ± 1.7 (^{68}Ga-**24**), 7.3 ± 2.0 (^{68}Ga-**22**), 7.1 ± 2.0 (^{68}Ga-**23**), 4.7 ± 1.4 (^{68}Ga-**30**). These results are comparable with in vitro experiments of ^{18}F-MISO, which show hypoxic (0.5% O_2) versus normoxic uptake ratios typically of 6:1.[5] Moreover, similar in vitro studies of previously reported ^{68}Ga-NOTA and -DOTA NI derivatives exhibited uptake ratios (hypoxic/normoxic) ranging from 1.5 to 5.6 after 60 min (in CHO, CT26, or Hela cell lines);[27,28] the uptake ratios of the four novel ^{68}Ga-(*CHX*)dedpa-NI tracers presented herein exhibited, on average, considerably higher values ranging from 4.7 to 7.3 after 60 min.

Overall there were no significant differences in uptake/retention between the four ^{68}Ga tracers tested in vitro, regardless of substitution of the nitro group on the imidazole ring (2-, 4-, or 5-NI), suggesting under the constraints of the in vitro assay the differences in the reduction potentials of the varying 2-, 4-, or 5-NI make no difference in the retention of the complexes in hypoxic cells. The overall uptake/retention is likely more critically controlled by the rate at which the tracers may diffuse inside the cell, which is traditionally regulated by the lipophilicity of the complexes. Indeed, all ^{68}Ga tracers exhibited similar log $D_{7.4}$ values ranging between −2.16 and −2.76 (vide supra). The lipophilic clinical hypoxia tracer ^{18}F-MISO is able to freely enter and exit cells through passive diffusion of the cell membrane; given the relatively hydrophilic nature of the ^{68}Ga-(*CHX*)dedpa-NI tracers tested herein, it may be conceivable that an alternate mode of cell uptake is available to the tracers, such as active transport. Nevertheless, further studies are required to discern the exact mechanism of radiotracer localization. The significantly higher uptake under

DOI: 10.1021/acs.inorgchem.5b00554
Inorg. Chem. 2015, 54, 4953−4965

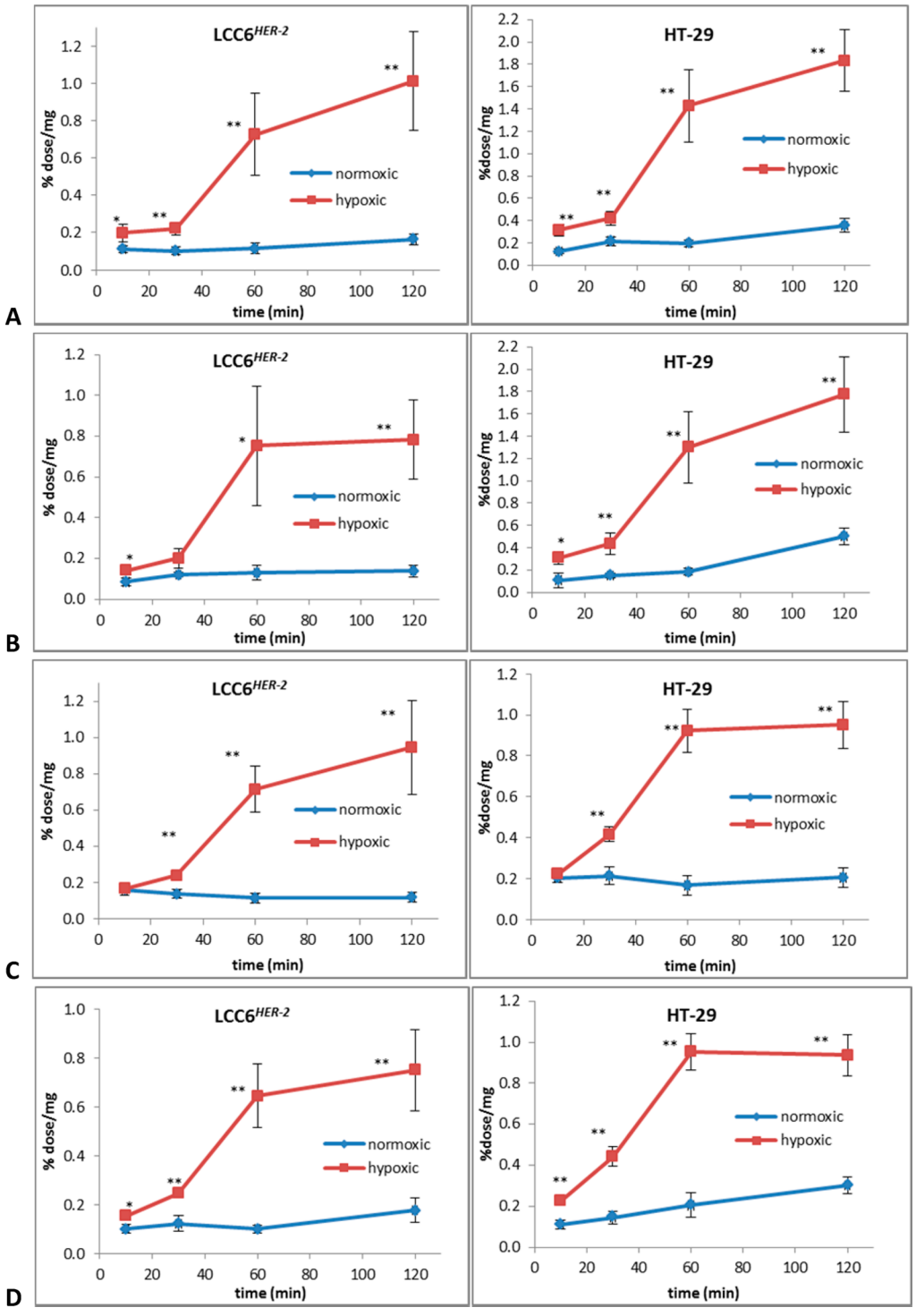

Figure 9. In vitro cell uptake studies of (A) ^{68}Ga-**22**, (B) ^{68}Ga-**23**, (C) ^{68}Ga-**24**, and (D) ^{68}Ga-**30** under normoxic (21% O_2, blue) and hypoxic (0.5% O_2, red) conditions in LCC6^{HER-2} and HT-29 cells. Statistical analyses of uptake ratios (hypoxic/normoxic) were performed using the Student's *t*-test (*, $p < 0.05$; **, $p < 0.01$; $n = 3$ at each time point).

hypoxic conditions than normoxic conditions for all four radioligands tested suggests that these ^{68}Ga-(*CHX*)dedpa-NI tracers would be promising candidates for further testing in vivo.

CONCLUSIONS

Nine NI-containing derivatives of the promising gallium(III) chelators H_2dedpa and H_2*CHX*dedpa were successfully synthesized and characterized. All chelating ligands retained their ability to quantitatively (RCY >99%) label $^{67/68}$Ga in 10 min at room temperature, a marked advantage over other NI-macrocyclic analogues such as NI-NOTA and NI-DOTA, which required heating at 100 °C to accomplish quantitative labeling of gallium isotopes.[27,28] Moreover, stability assays with *apo*-transferrin suggest that all propyl-linked H_2dedpa and H_2*CHX*dedpa analogues form kinetically inert gallium complexes, with stabilities ranging from 86 to >99% intact after a 2

DOI: 10.1021/acs.inorgchem.5b00554
Inorg. Chem. 2015, 54, 4953−4965

h *apo*-transferrin challenge assay. In vitro cell uptake of three $[^{68}Ga(dedpa\text{-}N,N'\text{-}propyl\text{-}NI)]^+$ tracers and one $[^{68}Ga(CHXdedpa\text{-}N,N'\text{-}propyl\text{-}NI)]^+$ complex with three cell lines, $LCC6^{HER\text{-}2}$, HT-29, and CHO, was tested under hypoxic (0.5% O_2) and normoxic conditions. All four ^{68}Ga tracers exhibited exceptional differentiation between hypoxic and normoxic uptake after 60 min, with ratios ranging from 4.7 to 7.9. The results suggest that these novel H_2dedpa- and H_2CHXdedpa-*N,N′*-alkyl-NI ligands would be ideal candidates for further testing in vivo for PET imaging of hypoxia with ^{68}Ga.

EXPERIMENTAL SECTION

Materials and Methods. All solvents and reagents were purchased from commercial suppliers (Sigma-Aldrich, TCI America, and Fisher Scientific) and were used as received. Human *apo*-transferrin was purchased from Sigma-Aldrich. The analytical thin-layer chromatography (TLC) plates were aluminum-backed ultrapure silica gel 60 with 250 μm thickness; the flash column silica gel (standard grade, 60 Å, 40−63 μm) was provided by Silicycle. ^1H and ^{13}C NMR spectra were recorded at 25 °C unless otherwise noted on a Bruker AV300, AV400, or AV600 instrument; NMR spectra are expressed on the δ scale and were referenced to residual solvent peaks. Low-resolution MS was performed using a Waters ZG spectrometer with an ESCI electrospray/chemical ionization source, and high-resolution electrospray ionization mass spectrometry (ESI-MS) was performed on a Micromass LCT time-of-flight instrument at the Department of Chemistry, University of British Columbia. ^{67}Ga-(chelate) human *apo*-transferrin stability experiments were analyzed using GE Healthcare Life Sciences PD-10 desalting columns (size exclusion for MW < 5000 Da) and counted with a Capintec CRC 15R well counter. The radioactivity of ^{68}Ga-labeled tracers for in vitro studies was measured using a Capintec CRC-25R/W dose calibrator. The high-performance liquid chromatography (HPLC) system used for analysis and purification of cold compounds consisted of a Waters 600 controller, a Waters 2487 dual-wavelength absorbance detector, and a Waters delta 600 pump. Phenomenex synergi hydro-RP 80 Å columns (250 mm × 4.6 mm analytical or 250 mm × 21.2 mm semipreparative) were used for the purification of several of the deprotected chelators. Analysis of radiolabeled complexes was carried out using either a Phenomenex hydro-RP 80 Å column (250 mm × 4.6 mm analytical) using a Waters Alliance HT 2795 separation module equipped with a Raytest Gabi Star NaI (Tl) detector and a Waters 996 photodiode array or a Phenomenex C18 column (5 μ, 250 × 10 mm) using an Agilent HPLC system equipped with a model 1200 quaternary pump, a model 1200 UV absorbance detector (set at 220 nm), and a Bioscan (Washington, DC) NaI scintillation detector (the radiodetector was connected to a Bioscan B-FC-1000 flow-count system, and the output from the Bioscan flow-count system was fed into an Agilent 35900E interface, which converted the analog signal to a digital signal). $^{67}GaCl_3$ was cyclotron-produced and provided by Nordion as a ∼0.1 M HCl solution. ^{68}Ga was obtained either from Nordion (5−10 mCi/mL) from a generator constructed of a titanium dioxide sorbent that was charged with ^{68}Ge and eluted with aqueous HCl (0.1 M)[40,41] or from an Eckert & Ziegler (Berlin, Germany) IGG100 ^{68}Ga generator and was purified according to previously published procedures[42] using a DGA resin column.

Compounds **1**−**3** and **1′**−**3′** were prepared as previously reported.[31,32]

*General Procedure for the Preparation of Nitroimidazole Potassium Salt (**4**, **5**, or **6**).* A calculated quantity of KOH in aqueous solution (1 mol equiv, 0.1 M) was added to NI, and the mixture was warmed to 60 °C to dissolve the imidazole. The water was removed in vacuo, and the imidazole salt was dried under vacuum at 115 °C overnight (100%).

*General Procedure for 1-(ω-Bromoalkyl)nitroimidazoles (**7**−**12**).* Compounds **7**−**12** were synthesized as per analogues reported in the literature.[33] The nitroimidazole potassium salt (**4**, **5**, or **6**; 1.3 mmol, 1 equiv) and 18-crown-6 (3.9 mmol, ∼3 equiv) dissolved in distilled CH_3CN (75 mL) were added dropwise to a refluxing solution of the appropriate 1,ω-dibromoalkane (13 mmol, 10 equiv) in distilled CH_3CN (100 mL) under N_2 over 1 h. The resultant solution was set at reflux for 16−24 h. The solvent was subsequently removed in vacuo, and the crude was purified by column chromatography (SiO_2, 3:1 EtOAc/petroleum ether).

*1-(3-Bromopropyl)-2-methyl-5-nitroimidazole (**7**).* Yield: beige solid (73%). ^1H NMR (400 MHz, $CDCl_3$): δ 7.68 (s, 1H), 4.06 (t, J = 6.8 Hz, 2H), 3.30 (t, J = 5.9 Hz, 2H), 2.33 (s, 3H), 2.29−2.14 (m, 2H). ^{13}C NMR (101 MHz, $CDCl_3$): δ 146.2, 144.8, 119.8, 44.8, 32.2, 28.9, 12.9.

*1-(3-Bromopropyl)-4-nitroimidazole (**8**).* Yield: beige solid (68%). ^1H NMR (400 MHz, $CDCl_3$): δ 7.81 (d, J = 1.3 Hz, 1H), 7.49 (d, J = 0.9 Hz, 1H), 4.27 (t, J = 6.6 Hz, 2H), 3.37 (t, J = 6.0 Hz, 2H), 2.43−2.31 (m, 2H). ^{13}C NMR (101 MHz, $CDCl_3$): δ 148.2, 136.2, 119.2, 46.0, 32.7, 28.7.

*1-(3-Bromopropyl)-2-nitroimidazole (**9**).* Yield: beige solid (74%). ^1H NMR (400 MHz, $CDCl_3$): δ 7.20 (s, 1H), 7.07 (s, 1H), 4.55 (t, J = 6.7 Hz, 2H), 3.33 (t, J = 6.1 Hz, 2H), 2.35 (p, J = 6.5 Hz, 2H). ^{13}C NMR (101 MHz, $CDCl_3$): δ 128.7, 126.9, 48.4, 32.5, 29.5.

*1-(2-Bromoethyl)-2-methyl-5-nitroimidazole (**10**).* Yield: beige solid (44%). ^1H NMR (300 MHz, $CDCl_3$): δ 7.79 (s, 1H), 4.36 (t, J = 6.0 Hz, 2H), 3.64 (t, J = 6.0 Hz, 2H), 2.44 (s, 3H).

*1-(2-Bromoethyl)-4-nitroimidazole (**11**).* Yield: white solid (51%). ^1H NMR (400 MHz, $CDCl_3$): δ 7.85 (d, J = 1.5 Hz, 1H), 7.52 (d, J = 1.3 Hz, 1H), 4.46 (t, J = 5.9 Hz, 2H), 3.67 (t, J = 5.9 Hz, 2H). ^{13}C NMR (101 MHz, $CDCl_3$): δ 136.2, 119.1. 49.6. 29.6.

*1-(2-Bromoethyl)-2-nitroimidazole (**12**).* Yield: yellow solid (56%). ^1H NMR (300 MHz, $CDCl_3$): δ 7.22 (s, 1H), 7.13 (s, 1H), 4.78 (t, J = 5.9 Hz, 2H), 3.72 (t, J = 5.9 Hz, 2H). ^{13}C NMR (101 MHz, $CDCl_3$): δ 128.3, 127.0. 51.3, 29.6.

*General Procedure for N,N′-Alkylation of Me_2dedpa (**13**−**18**).* Compound **3** (279 mg, 0.78 mmol) and the appropriate 1-(ω-bromoalkyl)nitroimidazole (**7**−**12**; 1.95 mmol, 2.5 equiv) was dissolved in CH_3CN (6 mL), and potassium carbonate (572 mg, 4.14 mmol, ∼5 equiv) was added. The reaction mixture was stirred at reflux for 2−3 days and subsequently cooled to room temperature, and inorganic salts were filtered out. The filtrate was concentrated in vacuo, and the crude oil was purified by column chromatography (CombiFlash R_f automated column system; 40 g of HP silica; A = dichloromethane, B = methanol, 100% A to 15% B gradient).

*Me_2dedpa-N,N′-ethyl-2-methyl-5-nitroimidazole (**13**).* Yield: yellow oil (23%). ^1H NMR (400 MHz, MeOD): δ 7.92 (dd, J = 7.9 and 5.4 Hz, 4H), 7.79 (s, 2H), 7.60 (dd, J = 5.5 and 3.0 Hz, 2H), 4.40 (s, 4H), 4.29 (t, J = 6.0 Hz, 4H), 3.82 (s, 6H), 3.60 (s, 4H), 3.54 (t, J = 5.9 Hz, 4H), 2.22 (s, 6H). ^{13}C NMR (101 MHz, MeOD): δ 166.3, 156.6, 148.1, 147.0, 146.8, 140.4, 128.8, 126.0, 122.3, 57.8, 55.2, 53.6, 52.3, 44.0, 12.8. MS (ES^+): m/z 665.5 ($[M + H]^+$).

*Me_2dedpa-N,N′-ethyl-4-nitroimidazole (**14**).* Yield: yellow oil (15%). ^1H NMR (300 MHz, MeOD): δ 8.09 (d, J = 1.2 Hz, 2H), 7.95 (d, J = 7.6 Hz, 2H), 7.80 (t, J = 7.7 Hz, 2H), 7.73 (d, J = 1.2 Hz, 2H), 7.33 (d, J = 7.6 Hz, 2H), 4.18 (t, J = 5.6 Hz, 4H), 3.96 (s, 6H), 3.80 (s, 4H), 3.37 (s, 3H), 2.89 (t, J = 5.6 Hz, 4H), 2.64 (s, 4H). MS (ES^-): m/z 715.5 ($[M + {}^{79}Br]^-$).

*Me_2dedpa-N,N′-ethyl-2-nitroimidazole (**15**).* Yield: yellow oil (10%). ^1H NMR (300 MHz, $CDCl_3$): δ 7.97 (d, J = 7.7 Hz, 2H), 7.72 (t, J = 7.7 Hz, 2H), 7.22 (s, 2H), 7.13 (d, J = 7.6 Hz, 2H), 7.03 (s, 2H), 4.50 (t, J = 5.5 Hz, 4H), 3.97 (s, 6H), 3.79 (s, 4H), 2.85 (t, J = 5.5 Hz, 4H), 2.57 (s, 4H). MS (ES^-): m/z 715.4 ($[M + {}^{79}Br]^-$).

*Me_2dedpa-N,N′-propyl-2-methyl-5-nitroimidazole (**16**).* Yield: yellow oil (34%). ^1H NMR (400 MHz, MeOD): δ 8.00 (s, 2H), 7.97 (d, J = 7.7 Hz, 2H), 7.89 (t, J = 7.7 Hz, 2H), 7.64 (d, J = 7.8 Hz, 2H), 4.03 (t, J = 7.1 Hz, 4H), 3.95 (s, 6H), 3.82 (s, 4H), 2.67 (s, 4H), 2.56 (t, J = 6.7 Hz, 4H), 2.36 (s, 6H), 2.05−1.93 (m, 4H). ^{13}C NMR (101 MHz, $CDCl_3$): δ 165.3, 159.4, 147.2, 145.9, 144.5, 137.4, 126.0, 123.6, 120.0, 59.6, 52.6, 51.9, 50.9, 44.6, 27.4, 12.8. MS (ES^+): m/z 693.4 ($[M + H]^+$).

*Me_2dedpa-N,N′-propyl-4-nitroimidazole (**17**).* Yield: yellow oil (30%). ^1H NMR (400 MHz, MeOD): δ 8.12 (d, J = 1.3 Hz, 2H), 7.95

DOI: 10.1021/acs.inorgchem.5b00554
Inorg. Chem. 2015, 54, 4953−4965

(dd, J = 7.6 and 0.7 Hz, 2H), 7.87 (t, J = 7.7 Hz, 2H), 7.74 (d, J = 1.3 Hz, 2H), 7.63 (dd, J = 7.7 and 0.7 Hz, 2H), 4.15 (t, J = 6.9 Hz, 4H), 3.95 (s, 6H), 3.78 (s, 4H), 2.62 (s, 4H), 2.51 (t, J = 6.7 Hz, 4H), 2.03 (p, J = 6.7 Hz, 4H). ^{13}C NMR (101 MHz, $CDCl_3$): δ 166.8, 161.6, 148.5, 148.1, 139.1, 138.4, 128.2, 124.7, 121.7, 60.6, 53.2, 53.1, 52.2, 47.2, 28.9. MS (ES^+): m/z 665.4 ($[M + H]^+$).

*Me_2dedpa-N,N′-propyl-2-nitroimidazole (**18**).* Yield: yellow oil (69%). ^{1}H NMR (400 MHz, $CDCl_3$): δ 7.85 (d, J = 7.4 Hz, 2H), 7.67 (t, J = 7.8 Hz, 2H), 7.45 (d, J = 7.5 Hz, 2H), 7.10 (d, J = 0.5 Hz, 2H), 6.93 (d, J = 0.6 Hz, 2H), 4.37−4.27 (m, 4H), 3.82 (s, 6H), 3.69 (s, 4H), 2.53 (s, 4H), 2.45 (t, J = 6.5 Hz, 4H), 1.93−1.82 (m, 4H). ^{13}C NMR (101 MHz, $CDCl_3$): δ 165.4, 159.9, 147.1, 144.4, 137.3, 128.0, 126.4, 126.0, 123.5, 70.3, 60.0, 52.6, 51.5, 48.1, 27.9. MS (ES^+): m/z 665.4 ($[M + H]^+$).

*General Procedure for Methyl Ester Deprotection of **13**−**18**.* The methyl ester protected ligand (**13**−**18**; 0.17 mmol) was dissolved in THF/water (3:1, 6 mL), and lithium hydroxide (20 mg, 0.83 mmol, 5 equiv) was added. The reaction mixture was stirred at ambient temperature until the reaction was complete by TLC (15−30 min). (R_f(products) = ∼0.06 in 10% methanol/dichloromethane.) The mixture was subsequently evaporated to dryness and purified by semipreparative HPLC (A, 0.1% trifluoroacetic acid in water; B, CH_3CN; 5−100% B; 30 min, 10 mL/min). Product fractions were pooled and lyophilized.

*H_2dedpa-N,N′-ethyl-2-methyl-5-nitroimidazole (**19**).* Yield: beige solid (66%). ^{1}H NMR (300 MHz, DMSO): δ 8.29 (s, 2H), 7.96 (dd, J = 8.3 and 5.2 Hz, 4H), 7.63 (dd, J = 5.8 and 2.7 Hz, 2H), 4.46−4.38 (m, 4H), 4.36 (s, 4H), 3.43 (s, 4H), 3.33 (t, J = 6.2 Hz, 4H), 2.30 (s, 6H). ^{13}C NMR (101 MHz, DMSO): δ 165.6, 154.3, 147.6, 145.3, 145.2, 138.6, 127.3, 124.1, 122.2, 56.7, 52.4, 49.4, 42.4, 12.6. HR-ESI-MS. Calcd (found) for $C_{28}H_{33}N_{10}O_8$ ($M + H^+$): m/z 637.2483 (637.2484).

*H_2dedpa-N,N′-ethyl-4-nitroimidazole (**20**).* Yield: yellow solid (98%). ^{1}H NMR (400 MHz, MeOD): δ 8.01 (d, J = 1.4 Hz, 2H), 7.95 (d, J = 7.5 Hz, 2H), 7.87 (t, J = 7.7 Hz, 2H), 7.63 (d, J = 1.5 Hz, 2H), 7.36 (d, J = 7.5 Hz, 2H), 4.22−4.08 (m, 4H), 3.91 (s, 4H), 2.77−2.67 (m, 4H), 2.46 (s, 4H). ^{13}C NMR (101 MHz, MeOD): δ 172.2, 159.0, 154.8, 148.6, 139.8, 138.4, 125.6, 123.2, 121.6, 60.3, 55.1, 52.0, 45.8. HR-ESI-MS. Calcd (found) for $C_{26}H_{29}N_{10}O_8$ ($M + H^+$): m/z 609.2170 (609.2178).

*H_2dedpa-N,N′-ethyl-2-nitroimidazole (**21**).* Yield: yellow solid (95%). ^{1}H NMR (400 MHz, MeOD): δ 7.95−7.87 (m, 4H), 7.40 (d, J = 6.5 Hz, 2H), 7.37 (d, J = 1.0 Hz, 2H), 7.06 (d, J = 1.0 Hz, 2H), 4.51−4.39 (m, 4H), 4.03 (s, 4H), 2.79−2.66 (m, 4H), 2.53 (s, 4H). ^{13}C NMR (101 MHz, MeOD): δ 172.2, 172.1, 158.9, 139.8, 135.4, 128.7, 128.6, 125.6, 123.2, 60.7, 54.9, 52.1. HR-ESI-MS. Calcd (found) for $C_{26}H_{29}N_{10}O_8$ ($M + H^+$): m/z 609.2170 (609.2177).

*H_2dedpa-N,N′-propyl-2-methyl-5-nitroimidazole (**22**).* Yield: white solid (99%). ^{1}H NMR (400 MHz, MeOD): δ 8.01 (d, J = 7.6 Hz, 2H), 7.94 (t, J = 7.7 Hz, 2H), 7.90 (s, 2H), 7.58 (d, J = 7.4 Hz, 2H), 4.38 (s, 4H), 4.00 (t, J = 7.1 Hz, 4H), 3.49 (s, 4H), 3.17−3.09 (m, 4H), 2.29 (s, 6H), 2.23−2.10 (m, 4H). ^{13}C NMR (101 MHz, MeOD): δ 167.1, 156.6, 149.0, 146.8, 140.1, 128.3, 125.9, 121.7, 58.0, 53.5, 51.6, 45.6, 26.8, 12.7. HR-ESI-MS. Calcd (found): for $C_{30}H_{37}N_{10}O_8$ ($M + H^+$): m/z 665.2796 (665.2792).

*H_2dedpa-N,N′-propyl-4-nitroimidazole (**23**).* Yield: yellow solid (99%). ^{1}H NMR (400 MHz, MeOD): δ 7.89 (d, J = 1.1 Hz, 2H), 7.85 (d, J = 7.6 Hz, 2H), 7.72 (t, J = 7.7 Hz, 2H), 7.49 (d, J = 1.1 Hz, 2H), 7.20 (d, J = 7.7 Hz, 2H), 3.77 (t, J = 6.9 Hz, 4H), 3.67 (s, 4H), 2.07 (s, 4H), 2.07−1.99 (m, 4H), 1.84−1.71 (m, 4H). ^{13}C NMR (101 MHz, MeOD): δ 172.2, 159.2, 154.7, 148.5, 139.7, 138.2, 125.4, 123.0, 121.4, 60.3, 51.8, 51.5, 47.6, 26.5. HR-ESI-MS. Calcd (found) for $C_{28}H_{33}N_{10}O_8$ ($M + H^+$): m/z 637.2483 (637.2483).

*H_2dedpa-N,N′-propyl-2-nitroimidazole (**24**).* Yield: white solid (83%). ^{1}H NMR (600 MHz, MeOD): δ 8.00 (d, J = 7.3 Hz, 2H), 7.95 (t, J = 7.7 Hz, 2H), 7.59 (d, J = 7.5 Hz, 2H), 7.38 (d, J = 0.7 Hz, 2H), 7.12 (d, J = 0.8 Hz, 2H), 4.45 (t, J = 7.2 Hz, 4H), 4.40 (s, 4H), 3.51 (s, 4H), 3.23−3.16 (m, 4H), 2.29−2.21 (m, 4H). ^{13}C NMR (151 MHz, MeOD): δ 167.3, 156.4, 148.7, 140.1, 128.8, 128.3, 128.3, 125.9, 58.3, 53.6, 51.6, 48.7, 27.1. HR-ESI-MS. Calcd (found) for $C_{28}H_{33}N_{10}O_8$ ($M + H^+$): m/z 637.2483 (637.2490).

*Me_2CHXdedpa-N,N′-propyl-2-methyl-5-nitroimidazole (**25**).* To a stirred solution of Me_2*CHX*dedpa (**3′**; 220 mg, 0.53 mmol) and **7** (331 mg, 1.33 mmol, 2.5 equiv) in CH_3CN (∼4 mL) was added diisopropylethylamine (462 μL, 2.65 mmol, 5 equiv), and the mixture was heated to reflux for 3 days. The solvent was then concentrated in vacuo, and the crude oil was purified by column chromatography (CombiFlash R_f automated column system; 24 g of HP silica; A = dichloromethane, B = methanol, 100% A to 10% B gradient) to give **25** as a yellow oil (120 mg, 30%). ^{1}H NMR (600 MHz, MeOD): δ 7.97−7.92 (m, 4H), 7.76 (s, 2H), 7.65 (dd, J = 7.1 and 1.1 Hz, 2H), 4.37 (d, J = 13.9 Hz, 2H), 3.93 (d, J = 14.0 Hz, 2H), 3.86 (t, J = 7.1 Hz, 4H), 3.56 (s, 6H), 3.55−3.52 (m, 2H), 3.16−3.06 (m, 4H), 2.27 (d, J = 11.5 Hz, 2H), 2.17−2.13 (m, 2H), 2.11 (s, 6H), 2.04 (tt, J = 12.1 and 6.0 Hz, 2H), 1.93 (d, J = 8.0 Hz, 2H), 1.68−1.59 (m, 2H), 1.46 (t, J = 9.5 Hz, 2H). ^{13}C NMR (151 MHz, MeOD): δ 165.8, 157.3, 149.1, 146.7, 139.9, 129.2, 125.9, 122.0, 62.4, 54.2, 53.1, 51.0, 45.6, 28.1, 25.6, 25.5, 12.6. MS (ES^+): m/z 747.6 ($[M + H]^+$).

*Me_2CHXdedpa-N,N′-propyl-4-nitroimidazole (**26**).* This compound was prepared like compound **25** above but with 1-(3-bromopropyl)-4-nitroimidazole (**8**) as the alkylating agent. Yield: yellow oil (20%). ^{1}H NMR (400 MHz, MeOD): δ 8.05−7.95 (m, 4H), 7.92 (d, J = 1.4 Hz, 2H), 7.65 (dd, J = 7.4 and 1.0 Hz, 2H), 7.51 (d, J = 1.4 Hz, 2H), 4.37 (d, J = 13.8 Hz, 2H), 4.05−3.99 (m, 4H), 3.96 (d, J = 13.9 Hz, 2H), 3.65 (s, 6H), 3.57 (d, J = 9.0 Hz, 2H), 3.20−3.03 (m, 4H), 2.29 (d, J = 12.1 Hz, 2H), 2.25−2.13 (m, 4H), 1.99 (d, J = 8.5 Hz, 2H), 1.74−1.59 (m, 2H), 1.51 (t, J = 10.0 Hz, 2H). ^{13}C NMR (101 MHz, MeOD): δ 165.7, 157.1, 139.9, 138.2, 129.2, 126.0, 121.5, 62.4, 54.0, 53.1, 51.0, 46.8, 28.3, 25.6, 25.6. MS (ES^+): m/z 719.6 ($[M + H]^+$).

*Me_2CHXdedpa-N,N′-propyl-2-nitroimidazole (**27**).* To a stirred solution of Me_2*CHX*dedpa (**3′**; 238 mg, 0.58 mmol) and **9** (340 mg, 1.45 mmol, 2.5 equiv) in CH_3CN (5 mL) was added potassium carbonate (481 mg, 3.48 mmol, 6 equiv). The reaction mixture was stirred at reflux for 2 days and subsequently cooled to room temperature, and inorganic salts were removed by vacuum filtration. The solvent was removed in vacuo, and the crude oil was purified by column chromatography (CombiFlash R_f automated column system; 24 g of HP silica; A = dichloromethane, B = methanol, 100% A to 10% B gradient) to give **27** as a yellow oil (257 mg, 62%). ^{1}H NMR (400 MHz, $CDCl_3$): δ 7.89 (dd, J = 7.4 and 0.7 Hz, 2H), 7.64 (t, J = 7.6 Hz, 2H), 7.59 (d, J = 7.0 Hz, 2H), 7.05 (s, 2H), 6.98 (d, J = 0.7 Hz, 2H), 4.38−4.20 (m, 4H), 3.93 (d, J = 15.0 Hz, 2H), 3.90 (s, 6H), 3.73 (d, J = 15.0 Hz, 2H), 2.68 (d, J = 8.2 Hz, 2H), 2.64−2.50 (m, 4H), 1.99−1.92 (m, 2H), 1.92−1.83 (m, 4H), 1.71 (d, J = 6.9 Hz, 2H), 1.22−1.03 (m, 4H). ^{13}C NMR (101 MHz, $CDCl_3$): δ 165.6, 161.5, 147.3, 144.7, 137.3, 128.3, 126.4, 126.2, 123.6, 61.8, 56.4, 52.8, 48.6, 47.4, 29.8, 26.6, 25.8. MS (ES^+): m/z 719.5 ($[M + H]^+$).

*General Procedure for Methyl Ester Deprotection of **25**−**27**.* The methyl-protected ligand (**25**−**27**; 0.16 mmol) was dissolved in THF/water (3:1, 5 mL), and lithium hydroxide (19 mg, 0.80 mmol, 5 equiv) was added. The reaction mixture was stirred at ambient temperature until the reaction was complete by TLC (15−30 min). (R_f(products) = ∼0.1 in 15% methanol/dichloromethane.) The mixture was subsequently evaporated to dryness and purified by semipreparative HPLC (A, 0.1% trifluoroacetic acid in water; B, CH_3CN; 5−100% B; 30 min, 10 mL/min). Product fractions were pooled and lyophilized to yield the pro-ligand as a white powder (99% recovery).

*H_2CHXdedpa-N,N′-propyl-2-methyl-5-nitroimidazole (**28**).* ^{1}H NMR (400 MHz, MeOD): δ 8.03 (d, J = 7.6 Hz, 2H), 7.94 (t, J = 7.7 Hz, 2H), 7.75 (s, 2H), 7.63 (d, J = 7.5 Hz, 2H), 4.41 (d, J = 14.1 Hz, 2H), 3.94 (d, J = 14.2 Hz, 2H), 3.86 (t, J = 7.2 Hz, 4H), 3.55 (d, J = 9.0 Hz, 2H), 3.18−3.04 (m, 4H), 2.28 (d, J = 11.5 Hz, 2H), 2.22 (d, J = 3.8 Hz, 1H), 2.15 (d, J = 1.5 Hz, 1H), 2.14 (s, 6H), 2.11−2.04 (m, 2H), 1.96 (d, J = 8.3 Hz, 2H), 1.71−1.59 (m, 2H), 1.48 (t, J = 9.6 Hz, 2H). ^{13}C NMR (101 MHz, MeOD): δ 166.7, 156.8, 150.0, 146.7, 139.9, 128.7, 126.2, 121.6, 101.4, 62.2, 54.4, 50.9, 45.7, 28.3, 25.6, 25.3, 12.6. HR-ESI-MS. Calcd (found) for $C_{34}H_{43}N_{10}O_8$ ($M + H^+$): m/z 719.3265 (719.3271).

DOI: 10.1021/acs.inorgchem.5b00554
Inorg. Chem. 2015, 54, 4953−4965

*H_2CHXdedpa-N,N′-propyl-4-nitroimidazole (**29**).* ^{1}H NMR (400 MHz, MeOD): δ 8.08 (d, J = 7.7 Hz, 2H), 7.97 (t, J = 7.7 Hz, 2H), 7.90 (s, 2H), 7.62 (d, J = 7.5 Hz, 2H), 7.48 (s, 2H), 4.40 (d, J = 13.9 Hz, 3H), 4.06−3.98 (m, 4H), 3.96 (d, J = 14.3 Hz, 2H), 3.56 (d, J = 8.6 Hz, 2H), 3.18−3.03 (m, 4H), 2.28 (d, J = 11.9 Hz, 2H), 2.25−2.15 (m, 4H), 2.03−1.96 (m, 2H), 1.75−1.60 (m, 2H), 1.55−1.45 (m, 2H). HR-ESI-MS. Calcd (found) for $C_{32}H_{39}N_{10}O_8$ (M + H$^+$): m/z 691.2952 (691.2957).

*H_2CHXdedpa-N,N′-propyl-2-nitroimidazole (**30**).* ^{1}H NMR (400 MHz, MeOD): δ 7.95 (d, J = 7.7 Hz, 2H), 7.86 (t, J = 7.7 Hz, 2H), 7.52 (d, J = 7.7 Hz, 2H), 7.11 (s, 2H), 6.91 (s, 2H), 4.35 (d, J = 14.2 Hz, 2H), 4.28−4.20 (m, 4H), 3.86 (d, J = 14.2 Hz, 2H), 3.49 (d, J = 8.8 Hz, 2H), 3.08 (dt, J = 12.8 and 7.8 Hz, 4H), 2.21 (d, J = 10.4 Hz, 2H), 2.11−2.01 (m, 4H), 1.93−1.84 (m, 2H), 1.64−1.52 (m, 2H), 1.44−1.36 (m, 2H). ^{13}C NMR (151 MHz, MeOD): δ 166.6, 156.7, 149.8, 139.9, 128.7, 128.5, 128.2, 126.1, 62.2, 54.3, 51.0, 48.7, 28.3, 25.6, 25.2. HR-ESI-MS. Calcd (found) for $C_{32}H_{39}N_{10}O_8$ (M + H$^+$): m/z 691.2952 (691.2952).

*General Procedure for Gallium Complexation of Pro-Ligands **19**−**24** and **28**−**30**.* The appropriate pro-ligand (**19**−**24** or **28**−**30**) (0.02 mmol) was dissolved in methanol/water (1:1, ∼1 mL), and the pH of the solution was adjusted to ∼1−2 with 0.1 M HCl(aq). To this clear solution was added a solution of $Ga(ClO_4)_3{\cdot}6H_2O$ (13 mg in 80 μL of water, 0.03 mmol, 1.5 equiv), at which time a white precipitate formed. The pH of the mixture was adjusted to 4−5 using 0.1 M NaOH(aq) and stirred at room temperature overnight to ensure quantitative complexation. The resultant white precipitate was collected by centrifugation (10 min, 4000 rpm), the filtrate was discarded, and the solid pellet was further dried under vacuum to yield the gallium complex as the perchlorate salt [Ga(L)][ClO_4].

*[Ga(**19**)][ClO_4].* Yield: white solid (65%). ^{1}H NMR (400 MHz, DMSO): δ 8.68 (t, J = 7.8 Hz, 2H), 8.35 (d, J = 7.6 Hz, 2H), 8.31 (s, 2H), 8.25 (d, J = 7.9 Hz, 2H), 4.94 (d, J = 17.5 Hz, 2H), 4.78 (d, J = 17.5 Hz, 2H), 4.52−4.41 (m, 2H), 4.40−4.28 (m, 2H), 3.38 (d, J = 8.0 Hz, 3H), 3.17−3.04 (m, 6H), 2.34 (s, 6H). ^{13}C NMR (101 MHz, DMSO): δ 162.1, 150.6, 146.8, 145.6, 145.4, 143.5, 127.8, 123.5, 122.0, 55.4, 50.1, 48.5, 12.8. HR-ESI-MS. Calcd (found) for $C_{28}H_{30}{}^{69}GaN_{10}O_8$ (M$^+$): m/z 703.1504 (703.1505).

*[Ga(**20**)][ClO_4].* Yield: white solid (70%). ^{1}H NMR (600 MHz, DMSO): δ 8.65 (t, J = 7.8 Hz, 2H), 8.40 (d, J = 1.0 Hz, 2H), 8.31 (d, J = 7.6 Hz, 2H), 8.20 (d, J = 8.0 Hz, 2H), 7.83 (d, J = 1.0 Hz, 2H), 4.84 (d, J = 17.5 Hz, 2H), 4.78 (d, J = 17.5 Hz, 2H), 4.58−4.51 (m, 2H), 4.44−4.35 (m, 2H), 3.17 (d, J = 11.4 Hz, 2H), 3.13−3.02 (m, 6H). ^{13}C NMR (151 MHz, DMSO): δ 162.1, 150.5, 147.0, 146.9, 143.6, 127.8, 123.6, 121.9, 55.4, 41.6. HR-ESI-MS. Calcd (found) for $C_{26}H_{26}{}^{69}GaN_{10}O_8$ (M$^+$): m/z 675.1191 (675.1183).

*[Ga(**21**)][ClO_4].* Yield: white solid (73%). ^{1}H NMR (400 MHz, DMSO): δ 8.65 (t, J = 7.8 Hz, 2H), 8.32 (d, J = 7.6 Hz, 2H), 8.23 (d, J = 7.9 Hz, 2H), 7.64 (s, 2H), 7.19 (s, 2H), 5.08−4.97 (m, 2H), 4.89 (d, J = 17.3 Hz, 2H), 4.73 (d, J = 17.5 Hz, 2H), 4.71−4.63 (m, 2H), 4.10 (dd, J = 10.1 and 5.0 Hz, 2H), 3.62 (d, J = 11.2 Hz, 2H), 3.25−3.19 (m, 2H), 3.04 (d, J = 11.3 Hz, 2H). ^{13}C NMR (151 MHz, DMSO): δ 162.1, 150.2, 146.9, 144.7, 143.6, 128.1, 127.9, 127.8, 123.4, 54.7, 49.6, 47.9, 42.9. HR-ESI-MS. Calcd (found) for $C_{26}H_{26}{}^{69}GaN_{10}O_8$ (M$^+$): m/z 675.1191 (675.1202).

*[Ga(**22**)][ClO_4].* Yield: beige solid (68%). ^{1}H NMR (400 MHz, DMSO): δ 8.69 (t, J = 7.8 Hz, 2H), 8.34 (d, J = 7.6 Hz, 2H), 8.20 (d, J = 8.0 Hz, 2H), 8.09 (s, 2H), 4.68−4.55 (m, 4H), 3.85 (t, J = 7.2 Hz, 4H), 3.18 (d, J = 10.8 Hz, 2H), 2.86 (d, J = 11.3 Hz, 2H), 2.77−2.59 (m, 4H), 2.30 (s, 6H), 2.23−2.10 (m, 2H), 2.08−1.94 (m, 2H). ^{13}C NMR (151 MHz, DMSO): δ 162.0, 150.7, 146.8, 145.5, 144.9, 143.7, 127.8, 123.3, 121.6, 55.6, 48.6, 47.9, 44.0, 23.0, 12.6. HR-ESI-MS. Calcd (found) for $C_{30}H_{34}{}^{69}GaN_{10}O_8$ (M$^+$): m/z 731.1817 (731.1812).

*[Ga(**23**)][ClO_4].* Yield: white solid (55%). ^{1}H NMR (400 MHz, DMSO): δ 8.68 (t, J = 7.8 Hz, 2H), 8.33 (d, J = 7.5 Hz, 2H), 8.25 (s, 1H), 8.18 (d, J = 7.9 Hz, 2H), 7.72 (s, 2H), 4.64 (d, J = 17.6 Hz, 2H), 4.56 (d, J = 17.5 Hz, 2H), 3.94 (t, J = 7.1 Hz, 4H), 3.17 (d, J = 11.0 Hz, 2H), 2.86 (d, J = 11.0 Hz, 2H), 2.77−2.65 (m, 2H), 2.65−2.54 (m, 2H), 2.31−2.17 (m, 2H), 2.16−2.01 (m, 2H). ^{13}C NMR (101 MHz, $CDCl_3$): δ 162.0, 150.6, 147.0, 146.7, 143.7, 137.1, 127.8, 123.3, 121.1, 55.6, 45.0, 23.3. HR-ESI-MS. Calcd (found) for $C_{28}H_{30}{}^{69}GaN_{10}O_8$ (M$^+$): m/z 703.1504 (703.1512).

*[Ga(**24**)][ClO_4].* Yield: off-white solid (58%). ^{1}H NMR (600 MHz, DMSO): δ 8.67 (t, J = 7.8 Hz, 2H), 8.36 (d, J = 7.6 Hz, 2H), 8.18 (d, J = 8.0 Hz, 2H), 7.33 (s, 2H), 7.14 (d, J = 0.7 Hz, 2H), 4.59 (q, J = 17.4 Hz, 4H), 4.40−4.32 (m, 2H), 4.22−4.14 (m, 2H), 3.16 (d, J = 11.4 Hz, 2H), 2.90−2.84 (m, 2H), 2.76−2.70 (m, 2H), 2.68−2.60 (m, 2H), 2.26−2.16 (m, 2H), 2.14−2.05 (m, 2H). ^{13}C NMR (151 MHz, DMSO): δ 162.0, 150.7, 146.6, 144.6, 143.8, 127.9, 127.8, 127.2, 123.3, 69.7, 55.4, 47.2, 40.1, 22.6. HR-ESI-MS. Calcd (found) for $C_{28}H_{30}{}^{69}GaN_{10}O_8$ (M$^+$): m/z 703.1504 (703.1497).

*[Ga(**28**)][ClO_4].* Yield: white solid (60%). ^{1}H NMR (400 MHz, DMSO): δ 8.66 (t, J = 7.8 Hz, 2H), 8.34 (d, J = 7.6 Hz, 2H), 8.15 (d, J = 7.9 Hz, 2H), 8.01 (s, 2H), 4.93 (d, J = 18.4 Hz, 2H), 4.46 (d, J = 18.4 Hz, 2H), 3.84−3.74 (m, 4H), 3.11 (d, J = 7.4 Hz, 2H), 2.69 (dt, J = 25.5 and 11.6 Hz, 4H), 2.77−2.60 (m, 4H), 2.24 (s, 6H), 2.18 (d, J = 10.8 Hz, 2H), 1.97 (dd, J = 10.7 and 6.2 Hz, 2H), 1.72 (d, J = 3.9 Hz, 4H), 1.38−1.28 (m, 2H), 1.24 (d, J = 8.0 Hz, 2H). ^{13}C NMR (101 MHz, DMSO): δ 161.9, 151.5, 146.9, 145.4, 144.9, 143.7, 126.5, 123.4, 121.4, 63.1, 54.7, 50.8, 44.0, 27.1, 25.5, 23.7, 12.5. HR-ESI-MS. Calcd (found) for $C_{34}H_{40}{}^{69}GaN_{10}O_8$ (M$^+$): m/z 785.2286 (785.2280).

*[Ga(**29**)][ClO_4].* Yield: white solid (78%). ^{1}H NMR (400 MHz, DMSO): δ 8.67 (t, J = 7.8 Hz, 2H), 8.34 (d, J = 7.6 Hz, 2H), 8.16 (s, 2H), 8.14 (d, J = 8.0 Hz, 2H), 7.64 (s, 2H), 4.94 (d, J = 18.4 Hz, 2H), 4.43 (d, J = 18.4 Hz, 2H), 3.98−3.79 (m, 4H), 3.11 (d, J = 7.5 Hz, 2H), 2.77−2.63 (m, 4H), 2.15 (d, J = 11.0 Hz, 2H), 2.10−1.97 (m, 2H), 1.81−1.63 (m, 4H), 1.43−1.27 (m, 2H), 1.27−1.13 (m, 2H). ^{13}C NMR (151 MHz, DMSO): δ 162.0, 151.5, 146.9, 143.7, 137.1, 126.6, 123.5, 121.2, 62.8, 54.9, 51.2, 45.1, 27.0, 26.0, 23.7. HR-ESI-MS. Calcd (found) for $C_{32}H_{36}{}^{69}GaN_{10}O_8$ (M$^+$): m/z 757.1973 (757.1976).

*[Ga(**30**)][ClO_4].* Yield: white solid (67%). ^{1}H NMR (600 MHz, DMSO): δ 7.71 (t, J = 7.8 Hz, 2H), 7.41 (d, J = 7.6 Hz, 2H), 7.18 (d, J = 7.9 Hz, 2H), 6.34 (s, 2H), 6.14 (d, J = 0.8 Hz, 2H), 3.96 (d, J = 18.4 Hz, 2H), 3.47 (d, J = 18.5 Hz, 4H), 3.28−3.23 (m, 6H), 2.14 (d, J = 8.9 Hz, 6H), 1.77 (d, J = 8.9 Hz, 8H), 1.19 (d, J = 11.1 Hz, 4H), 1.16−1.05 (m, 4H), 0.88−0.80 (m, 4H), 0.76 (d, J = 7.1 Hz, 4H), 0.39 (s, 4H), 0.27 (d, J = 14.5 Hz, 6H). ^{13}C NMR (151 MHz, DMSO): δ 162.1, 151.6, 147.0, 144.6, 143.8, 128.0, 127.3, 126.7, 123.6, 69.8, 63.1, 55.1, 51.0, 47.3, 27.2, 25.5, 23.7. HR-ESI-MS. Calcd (found) for $C_{32}H_{36}{}^{69}GaN_{10}O_8$ (M$^+$): m/z 757.1973 (757.1981).

X-ray Crystallography. A pink prism crystal of $C_{26}H_{26}GaN_{10}O_8{\cdot}ClO_4$, [Ga(**21**)][$ClO_4$], having approximate dimensions of 0.14 × 0.18 × 0.28 mm was mounted on a glass fiber. All measurements were made on a Bruker X8 APEX II diffractometer with graphite-monochromated Mo Kα radiation. The data were collected at a temperature of −173.0 ± 0.1 °C to a maximum 2θ value of 60.1°. Data were collected in a series of ϕ and ω scans in 0.50° oscillations with 15.0 s exposures. The crystal-to-detector distance was 39.99 mm. Data were collected and integrated using the Bruker *SAINT*[43] software package. Data were corrected for absorption effects using the multiscan technique (*SADABS*[44]), with minimum and maximum transmission coefficients of 0.800 and 0.855, respectively. The data were corrected for Lorentz and polarization effects. The structure was solved by direct methods.[45] The complex resides on a 2-fold rotation axis passing through the gallium atom, and thus has half of a molecule in the asymmetric unit. Additionally, the perchlorate anion is also disordered about a second 2-fold rotation axis. All non-hydrogen atoms were refined anisotropically. All hydrogen atoms were placed in calculated positions.

A colorless tablet crystal of $C_{28}H_{30}GaN_{10}O_{12}Cl$, [Ga(**23**)][$ClO_4$], having approximate dimensions of 0.08 × 0.25 × 0.25 mm was mounted on a glass fiber. All measurements were made on a Bruker X8 APEX II diffractometer with graphite-monochromated Mo Kα radiation. The data were collected at a temperature of −173.0 ± 0.1 °C to a maximum 2θ value of 58.4°. Data were collected in a series of ϕ and ω scans in 0.50° oscillations with 20.0 s exposures. The crystal-to-detector distance was 40.08 mm. Data were collected and integrated using the Bruker *SAINT*[43] software package. Data were corrected for absorption effects using the multiscan technique (*SADABS*[44]), with minimum and maximum transmission coefficients of 0.760 and 0.931,

DOI: 10.1021/acs.inorgchem.5b00554
Inorg. Chem. 2015, 54, 4953−4965

respectively. The data were corrected for Lorentz and polarization effects. The structure was solved by direct methods.[45] The material crystallizes with significant disorder to both the complex and ClO_4 counterion. Additional regions of unresolvable electron density were treated by the *PLATON/SQUEEZE*[46] program to generate a "solvent-free" data set. The amount of electrons removed from the entire cell (203) is consistent with approximately 1 solvent CH_3CN molecule per asymmetric unit. All non-hydrogen atoms were refined anisotropically. All hydrogen atoms were placed in calculated positions.

Electrochemical Studies. The CVs were measured using a potentiostat (PINE Instrument Company model AFCBP1 visualized with *AfterMath* software) at ambient temperature. All experiments were conducted in a one-compartment 3 mL cell; oxygen was removed by bubbling N_2 gas through the solution prior to taking measurements. Nonaqueous cyclic voltammetry was conducted with a platinum mesh counter electrode, a platinum wire working electrode, and a silver wire pseudoreference electrode. In addition, 0.10 M NBu_4ClO_4 in DMSO was used as the electrolyte solution. Ferrocene was added as an internal potential reference. For aqueous CVs, a platinum mesh counter electrode, a glass carbon working electrode (~2 mm diameter), and a saturated AgCl in KCl reference electrode were used. The electrolyte solution was 0.10 M KCl (pH 7) in water. Before use, the working electrode was polished with 0.25 and 0.05 μm diamond polishing paste, rinsed thoroughly with deionized water, then rinsed with methanol, and left to air dry. In most experiments, a 50 μL solution of compound in DMSO was added to 3 mL of the electrolyte solution in the cell to give measurement concentrations of 1−5 mM. CVs were recorded at 100 mV/s.

Radiochemistry. *$^{67/68}$Ga-Radiolabeling Studies.* For initial labeling studies and human *apo*-transferrin challenge assays, all chelators were made up as stock solutions (1 mg/mL, ~10^{-3} M) in deionized water. A 100 μL aliquot of each chelator stock solution was transferred to screw-cap MS vials and diluted with a pH 4 NaOAc (10 mM for ^{67}Ga or 100 mM for ^{68}Ga) buffer such that the final volume was 1 mL after the addition of $^{67/68}GaCl_3$, to a final chelator concentration of ~10^{-4} M for each sample. An aliquot of $^{67/68}GaCl_3$ (~1 mCi for labeling studies and ~3−6 mCi for *apo*-transferrin competitions) was added to the vials containing the chelator, allowed to radiolabel at ambient temperature for 10 min, and then analyzed by reversed-phase HPLC to confirm radiolabeling and calculate the yields. Areas under the peaks observed in the HPLC radiotrace were integrated to determine radiolabeling yields. Elution conditions used for reversed-phase HPLC analysis were as follows: A, 10 mM NaOAc buffer, pH 4.5; B, CH_3CN; 0−100% B linear gradient 20 min for [^{67}Ga(dedpa-*N*,*N*′-alkyl-NI)]$^+$ ([^{67}Ga(**19**−**24**)]$^+$; t_R = 8.2−9.4 min), [^{67}Ga-(*CHX*dedpa-*N*,*N*′-alkyl-NI)]$^+$ ([^{67}Ga(**28**−**30**)]$^+$; t_R = 10.1−11.0 min), and free ^{67}Ga (t_R = 2.4−3.1 min). The preparation of ^{68}Ga tracers for log $D_{7.4}$ and in vitro studies was accomplished by adding a $^{68}GaCl_3$ solution (0.5 mL in water) to a 4 mL glass vial preloaded with 0.7 mL of *N*-2-hydroxyethylpiperazine-*N*′-2-ethanesulfonic acid buffer (2 M, pH 5.0) and precursor (100 μg) and allowing it to radiolabel at ambient temperature for 10 min. No further purification was necessary.

Human *apo*-Transferrin Stability Data. The procedures closely followed those of a previously published method.[32,47] The radiolabeled complexes [^{67}Ga(**19**−**24** or **28**−**30**)]$^+$ were prepared with the radiolabeling protocol as described above. In triplicate, for each ^{67}Ga complex above, solutions were prepared in vials with 500 μL of freshly prepared 1 mg/mL *apo*-transferrin in a $NaHCO_3$ (10 mM, pH 7) solution, 300 μL of ^{67}Ga complex, and 200 μL of PBS (pH 7.4) and incubated at 37 °C in a water bath. At time points of 10 min and 1 and 2 h, 300 μL of the *apo*-transferrin competition mixture was removed from each vial, diluted to a total volume of 2.5 mL with PBS, and then counted in a Capintec CRC 15R well counter to obtain a value for the total activity to be loaded on the PD-10 column (F). The 2.5 mL of diluted *apo*-transferrin mixture was loaded onto a PD-10 column that had previously been conditioned via elution with 20 mL of PBS, and the empty vial was counted in a well counter to determine the residual activity left in the vial (R). The 2.5 mL of loading volume was allowed to elute into a waste container, and then the PD-10 column was eluted with 3.5 mL of PBS and collected into a separate vial. The eluent, which contained ^{67}Ga bound/associated with *apo*-transferrin (size exclusion for MW < 5000 Da), was counted in a well counter (E) and then compared to the total amount of activity that was loaded on the PD-10 column to obtain the percentage of ^{67}Ga that was bound to *apo*-transferrin and therefore no longer chelate-bound using eq 1.

$$\left(1 - \frac{E}{F - R}\right) \times 100 \quad (1)$$

Partition Coefficients. ^{68}Ga-labeled complex (30 μCi/6 μL) was added to 1.5 mL centrifuge tubes containing PBS (494 μL) and 1-octanol (500 μL), mixed vigorously for 1 min, and subsequently centrifuged to separate phases (3000 rpm, 5 min). Aliquots (100 μL) of the organic and aqueous phases were transferred and the radioactivities counted in a γ-counter (Packard Cobra II Auto Gamma). Measurements were carried out in triplicate.

In Vitro Cell Uptake Study. Cell uptake studies were carried out using LCC6^{HER-2}, HT-29, and CHO cell lines. LCC6^{HER-2} cells were maintained in a Dulbecco's modified Eagle medium (DMEM) culture medium enriched with 10% fetal bovine serum (FBS) containing 500 μg/mL G148 (Geneticin) (all from Invitrogen), HT-29 cells were maintained in McCoy's 5A medium enriched with 10% FBS, and CHO cells were maintained in DMEM with 10% FBS. All cell lines were maintained in 5% CO_2 in an incubator at 37 °C. For normoxic experiments, cells were subcultured for 24 h in 24-well plates (2×10^5 cells/well of HT-29 and CHO and 1×10^5 cells/well of LCC6^{HER-2}). For hypoxic experiments, cells were subcultured in 24-well plates as above for 20 h and then transferred to a hypoxia chamber (maintained at 0.5% O_2; remainder of 95% N_2 and 5% CO_2), the culture medium was replaced with fresh media that had been allowed to equilibrate under hypoxic conditions overnight, and then the cells were preincubated for 4 h under hypoxic conditions. ^{68}Ga-L_n (5 μCi/100 μL) was added to each well and incubated for 10, 30, 60, or 120 min; samples were carried out in triplicate. The medium was then decanted off, the wells were washed three times with PBS, and all washings were collected in counting tubes (W). The cells were then lifted with the addition of trypsin and quantitatively transferred to counting tubes (C). The tracer uptakes were measured using a γ-counter. The percentage uptake was calculated using eq 2.

$$\left(\frac{C}{C + W}\right) \times 100 \quad (2)$$

Each cell sample (C) was then pelleted and lysed (0.5 mL lysis buffer), and the total protein concentrations in the samples were determined using the bicinchoninic acid method (Pierce).

■ ASSOCIATED CONTENT

Supporting Information

^{1}H/^{13}C COSY NMR spectra of several precursors, ligands, and gallium complexes, CV of a representative [Ga(dedpa-*N*,*N*′-alkyl-NI)]$^+$ complex with the addition of 1 equiv of ferrocene (DMSO), CVs of selected Ga complexes in aqueous solvent (water), HPLC radiotraces of selected ^{67}Ga-labeled complexes, and crystallographic information files (CIF) for the X-ray structures along with relevant distance and bond angle data. This material is available free of charge via the Internet at http://pubs.acs.org.

■ AUTHOR INFORMATION

Corresponding Author

*E-mail: orvig@chem.ubc.ca. Phone: (604) 822-4449. Fax: (604) 822-2847.

Notes

The authors declare no competing financial interest.

DOI: 10.1021/acs.inorgchem.5b00554
Inorg. Chem. 2015, 54, 4953−4965

■ ACKNOWLEDGMENTS

We acknowledge Nordion (Canada) and the Natural Sciences and Engineering Research Council (NSERC) of Canada for grant support (CR&D, Discovery), the NSERC for CGS-M/CGS-D fellowships (to C.F.R.), and the University of British Columbia for 4YF fellowships (to C.F.R.). C.O. acknowledges the Canada Council for the Arts for a Killam Research Fellowship (2011−2013). The authors also thank Dr. Dennis W. Wester (Nordion) for collaboration throughout the project.

■ REFERENCES

(1) Krohn, K. A.; Link, J. M.; Mason, R. P. *J. Nucl. Med.* **2008**, *49* (Suppl 2), 129S−148S.
(2) Peitzsch, C.; Perrin, R.; Hill, R. P.; Dubrovska, A.; Kurth, I. *Int. J. Radiat. Biol.* **2014**, *90* (8), 636−652.
(3) Lucignani, G. *Eur. J. Nucl. Med. Mol. Imaging* **2008**, *35* (4), 838−842.
(4) Wilson, W. R.; Hay, M. P. *Nat. Rev. Cancer* **2011**, *11* (6), 393−410.
(5) Carlin, S.; Humm, J. L. *J. Nucl. Med.* **2012**, *53* (8), 1171−1174.
(6) Chitneni, S. K.; Palmer, G. M.; Zalutsky, M. R.; Dewhirst, M. W. *J. Nucl. Med.* **2011**, *52* (2), 165−168.
(7) Okuda, K.; Okabe, Y.; Kadonosono, T.; Ueno, T.; Youssif, B. G. M.; Kizaka-Kondoh, S.; Nagasawa, H. *Bioconjugate Chem.* **2012**, *23* (3), 324−329.
(8) Horsman, M. R.; Mortensen, L. S.; Petersen, J. B.; Busk, M.; Overgaard, J. *Nat. Rev. Clin. Oncol.* **2012**, *9* (12), 674−687.
(9) Nunn, A.; Linder, K.; Strauss, H. W. *Eur. J. Nucl. Med. Mol. Imaging* **1995**, *22* (3), 265−280.
(10) Padhani, A. R.; Krohn, K. A.; Lewis, J. S.; Alber, M. *Eur. Radiol.* **2007**, *17* (4), 861−872.
(11) Edwards, D. I. *J. Antimicrob. Chemother.* **1993**, *31* (1), 9−20.
(12) McClelland, R. A.; Panicucci, R.; Rauth, A. M. *J. Am. Chem. Soc.* **1987**, *109* (14), 4308−4314.
(13) Hicks, R. J.; Rischin, D.; Fisher, R.; Binns, D.; Scott, A. M.; Peters, L. J. *Eur. J. Nucl. Med. Mol. Imaging* **2005**, *32* (1), 1384−1391.
(14) Eschmann, S.; Paulsen, F.; Reimold, M.; Dittmann, H.; Welz, S.; Reischl, G.; Machulla, H.; Bares, R. *J. Nucl. Med.* **2005**, *46* (2), 253−260.
(15) Picchio, M.; Beck, R.; Haubner, R.; Seidl, S.; Machulla, H.-J.; Johnson, T. D.; Wester, H.-J.; Reischl, G.; Schwaiger, M.; Piert, M. *J. Nucl. Med.* **2008**, *49*, 597−605.
(16) Piert, M.; Machulla, H.; Picchio, M.; Reischl, G.; Ziegler, S.; Kumar, P.; Beck, R.; Mcewan, A. J. B.; Wiebe, L. I.; Schwaiger, M. *J. Nucl. Med.* **2005**, *46* (1), 106−113.
(17) Chitneni, S. K.; Bida, G. T.; Zalutsky, M. R.; Dewhirst, M. W. *J. Nucl. Med.* **2014**, *55* (7), 1192−1198.
(18) Komar, G.; Seppänen, M.; Eskola, O.; Lindholm, P.; Grönroos, T. J.; Forsback, S.; Sipilä, H.; Evans, S. M.; Solin, O.; Minn, H. *J. Nucl. Med.* **2008**, *49* (12), 1944−1951.
(19) Evans, S. M.; Kachur, A. V.; Shiue, C. Y.; Hustinx, R.; Jenkins, W. T.; Shive, G. G.; Karp, J. S.; Alavi, A.; Lord, E. M.; Dolbier, W. R.; Koch, C. J. *J. Nucl. Med.* **2000**, *41* (2), 327−336.
(20) Brown, J. M.; Workman, P. *Radiat. Res.* **1980**, *82* (1), 171−190.
(21) Wadas, T. J.; Wong, E. H.; Weisman, G. R.; Anderson, C. J. *Chem. Rev.* **2010**, *110* (5), 2858−2902.
(22) Ramogida, C. F.; Orvig, C. *Chem. Commun.* **2013**, *49* (42), 4720−4739.
(23) Green, M. A.; Welch, M. J. *Int. J. Rad. Appl. Instrum. B* **1989**, *16* (5), 435−448.
(24) Bartholomä, M. D.; Louie, A. S.; Valliant, J. F.; Zubieta, J. *Chem. Rev.* **2010**, *110* (5), 2903−2920.
(25) Fani, M.; Andre, J. P.; Maecke, H. R. *Contrast Media Mol. Imaging* **2008**, *3* (2), 53−63.
(26) Price, E. W.; Orvig, C. *Chem. Soc. Rev.* **2014**, *43* (1), 260−290.
(27) Hoigebazar, L.; Jeong, J. M.; Choi, S. Y.; Choi, J. Y.; Shetty, D.; Lee, Y.-S.; Lee, D. S.; Chung, J.-K.; Lee, M. C.; Chung, Y. K. *J. Med. Chem.* **2010**, *53* (17), 6378−6385.
(28) Hoigebazar, L.; Jeong, J. M.; Hong, M. K.; Kim, Y. J.; Lee, J. Y.; Shetty, D.; Lee, Y.-S.; Lee, D. S.; Chung, J.-K.; Lee, M. C. *Bioorg. Med. Chem.* **2011**, *19* (7), 2176−2181.
(29) Fernández, S.; Dematteis, S.; Giglio, J.; Cerecetto, H.; Rey, A. *Nucl. Med. Biol.* **2013**, *40* (2), 273−279.
(30) Boros, E.; Ferreira, C. L.; Cawthray, J. F.; Price, E. W.; Patrick, B. O.; Wester, D. W.; Adam, M. J.; Orvig, C. *J. Am. Chem. Soc.* **2010**, *132* (44), 15726−15733.
(31) Ramogida, C. F.; Cawthray, J. F.; Boros, E.; Ferreira, C. L.; Patrick, B. O.; Adam, M. J.; Orvig, C. *Inorg. Chem.* **2015**, *54* (4), 2017−2031.
(32) Price, E.; Zeglis, B.; Cawthray, J. F.; Ramogida, C. F.; Ramos, N.; Lewis, J. S.; Adam, M. J.; Orvig, C. *J. Am. Chem. Soc.* **2013**, *135* (34), 12707−12721.
(33) Long, A.; Parrick, J.; Hodgkiss, R. *Synthesis* **1991**, *9*, 709−713.
(34) Squella, J. A.; Núñez-Vergara, L. J.; Campero, a.; Maraver, J.; Jara-Ulloa, P.; Carbajo, J. *J. Electrochem. Soc.* **2007**, *154* (4), F77−F81.
(35) Valdez, C.; Tripp, J. *J. Med. Chem.* **2009**, *52* (13), 4038−4053.
(36) Wagh, N. K.; Zhou, Z.; Ogbomo, S. M.; Shi, W.; Brusnahan, S. K.; Garrison, J. C. *Bioconjugate Chem.* **2012**, *23* (3), 527−537.
(37) Huang, H.; Mei, L.; Chu, T. *Molecules* **2012**, *17* (6), 6808−6820.
(38) Bollo, S.; Jara-Ulloa, P.; Zapata-Torres, G.; Cutiño, E.; Sturm, J. C.; Núñez-Vergara, L. J.; Squella, J. a. *Electrochim. Acta* **2010**, *55* (15), 4558−4566.
(39) Harris, W. R.; Pecoraro, V. L. *Biochemistry* **1983**, *22* (2), 292−299.
(40) Ferreira, C. L.; Lamsa, E.; Woods, M.; Duan, Y.; Fernando, P.; Bensimon, C.; Kordos, M.; Guenther, K.; Jurek, P.; Kiefer, G. E. *Bioconjugate Chem.* **2010**, *21* (3), 531−536.
(41) Malyshev, K. V.; Smirnov, V. V. *Radiokhimiya* **1975**, *17*, 137−140.
(42) Lin, K.-S.; Pan, J.; Amouroux, G.; Turashvili, G.; Mesak, F.; Hundal-Jabal, N.; Pourghiasian, M.; Lau, J.; Jenni, S.; Aparicio, S.; Benard, F. *Cancer Res.* **2015**, *75* (2), 387−393.
(43) *SAINT*, version 7.60A; Bruker AXS Inc.: Madison, WI, 1997−2010.
(44) *SADABS*, version 2008/1; Bruker AXS Inc.: Madison, WI, 2008.
(45) Altomare, A.; Burla, M. C.; Camalli, M.; Cascarano, G. L.; Giacovazzo, C.; Guagliardi, A.; Moliterni, A. G. G.; Polidori, G.; Spagna, R. *J. Appl. Crystallogr.* **1999**, *32* (1), 115−119.
(46) Van der Sluis, P.; Spek, A. L. *Acta Crystallogr., Sect. A: Found. Crystallogr.* **1990**, *46* (3), 194−201.
(47) Price, E. W.; Cawthray, J. F.; Bailey, G.; Ferreira, C. L.; Boros, E.; Adam, M. J.; Orvig, C. *J. Am. Chem. Soc.* **2012**, *134* (20), 8670−8683.

DOI: 10.1021/acs.inorgchem.5b00554
Inorg. Chem. 2015, 54, 4953−4965